



(19) **United States**

(12) **Patent Application Publication**
Kar et al.

(10) **Pub. No.: US 2012/0051378 A1**
(43) **Pub. Date: Mar. 1, 2012**

(54) **PHOTODETECTION**

H01L 27/146 (2006.01)

H01L 21/268 (2006.01)

H01J 40/00 (2006.01)

G01J 1/42 (2006.01)

(76) Inventors: **Aravinda Kar**, Oviedo, FL (US);
Tariq Manzur, Newport, RI (US)

(21) Appl. No.: **12/964,072**

(52) **U.S. Cl.** **372/38.01**; 250/200; 250/216;
356/218; 257/77; 438/535; 438/29; 257/E27.133;
257/E21.347; 257/E21.09

(22) Filed: **Dec. 9, 2010**

Related U.S. Application Data

(60) Provisional application No. 61/378,498, filed on Aug. 31, 2010.

Publication Classification

(51) **Int. Cl.**

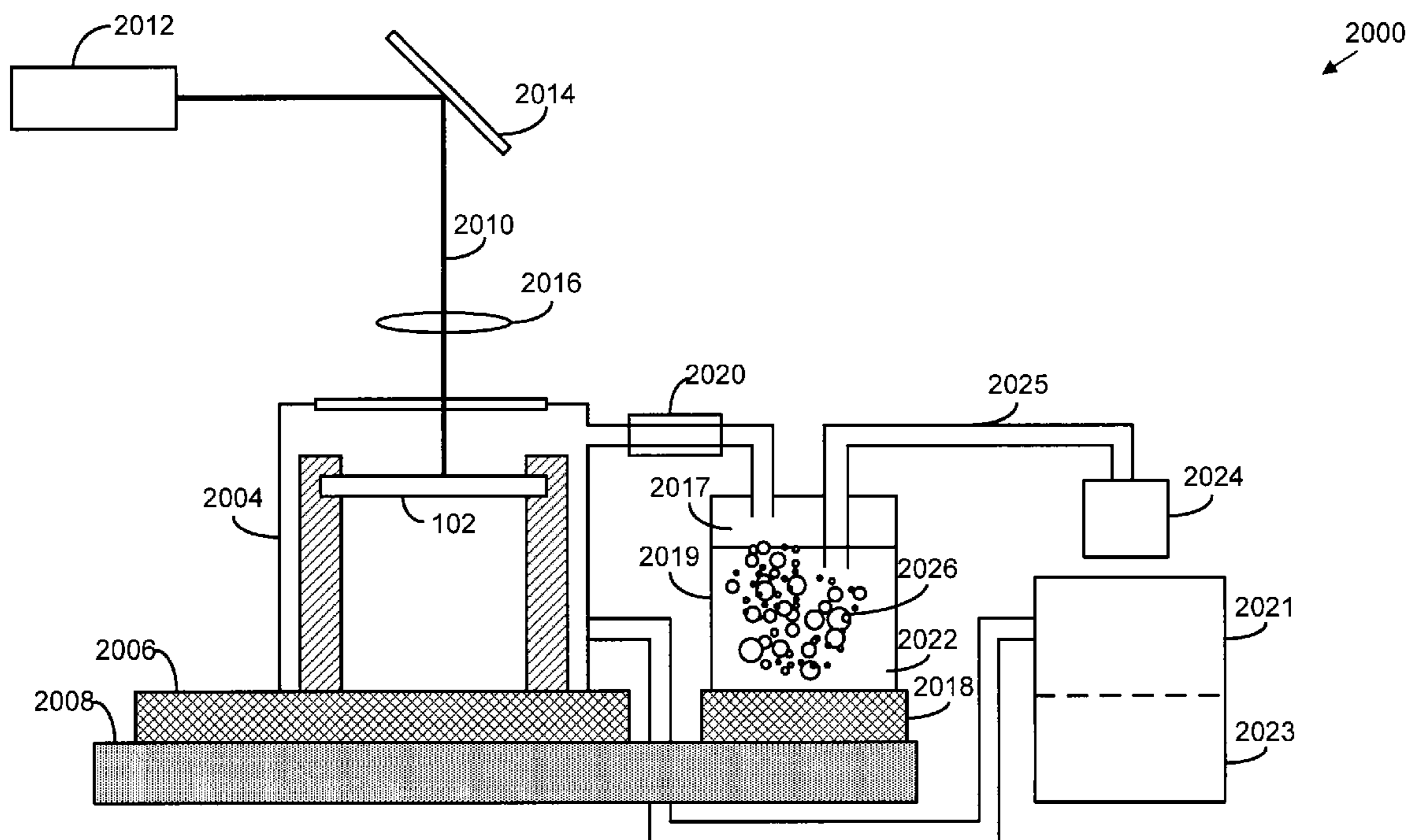
H01S 3/10 (2006.01)

H01J 40/14 (2006.01)

H01L 21/20 (2006.01)

(57) **ABSTRACT**

Embodiments of the present disclosure provide systems, devices, and methods for photodetection. For example, briefly described, in one embodiment among others, a sensor comprises an array of photodetectors, wherein the reflectance of each of the photodetectors is a function of the number of photons incident on the respective photodetector; and an electrical insulator positioned between one of the photodetectors and another one of the photodetectors to reduce diffusion of electrons therebetween.



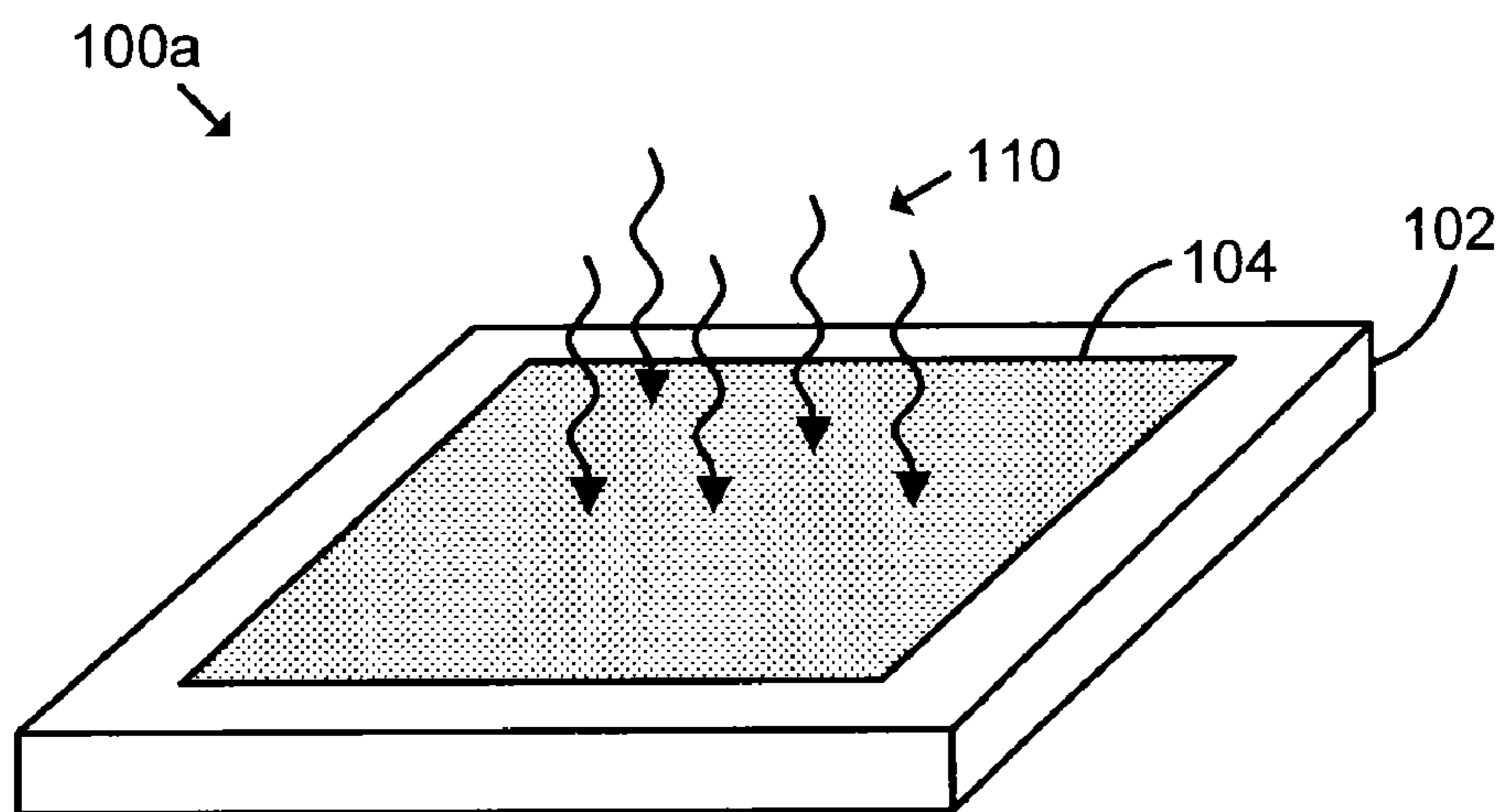


FIG. 1

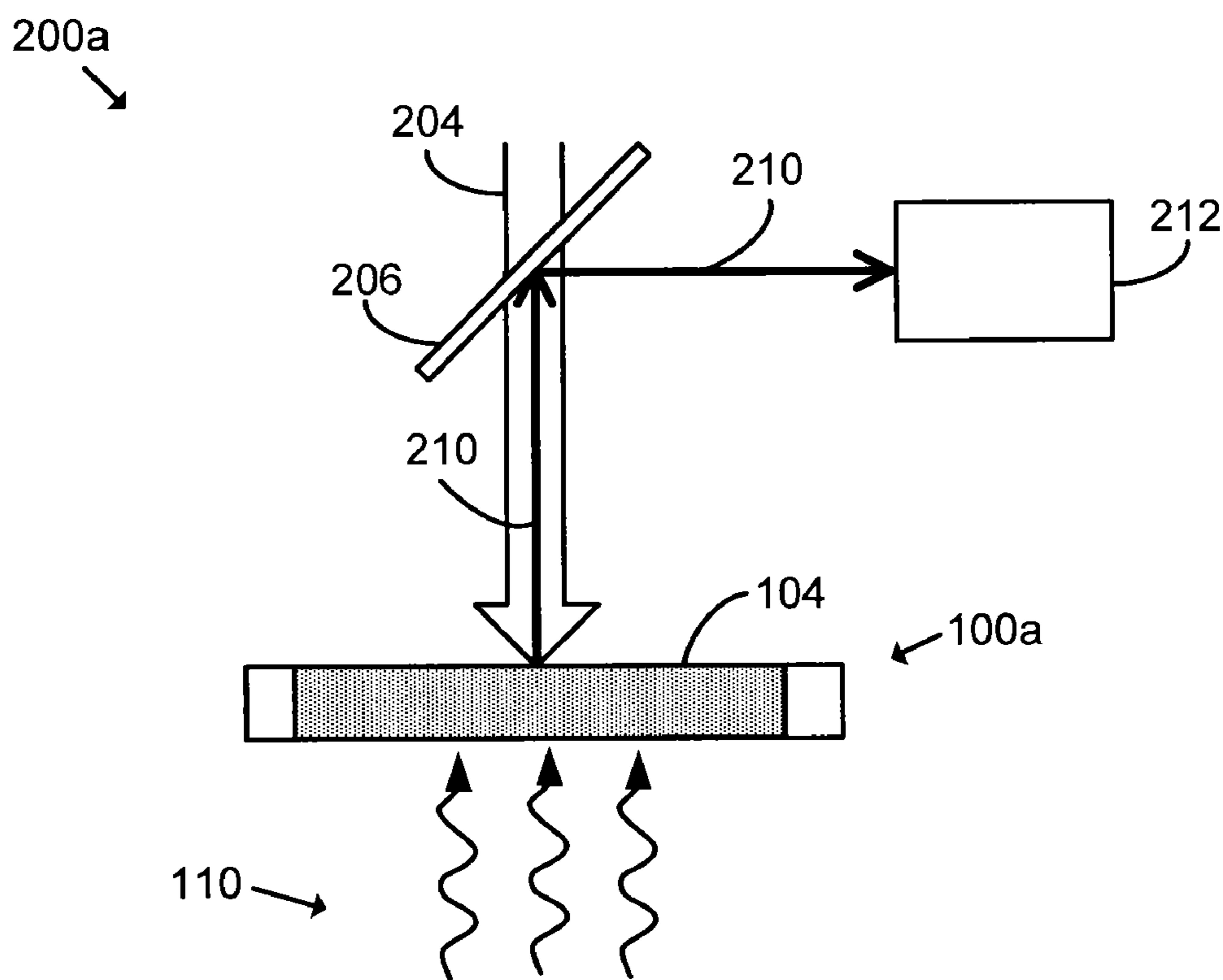
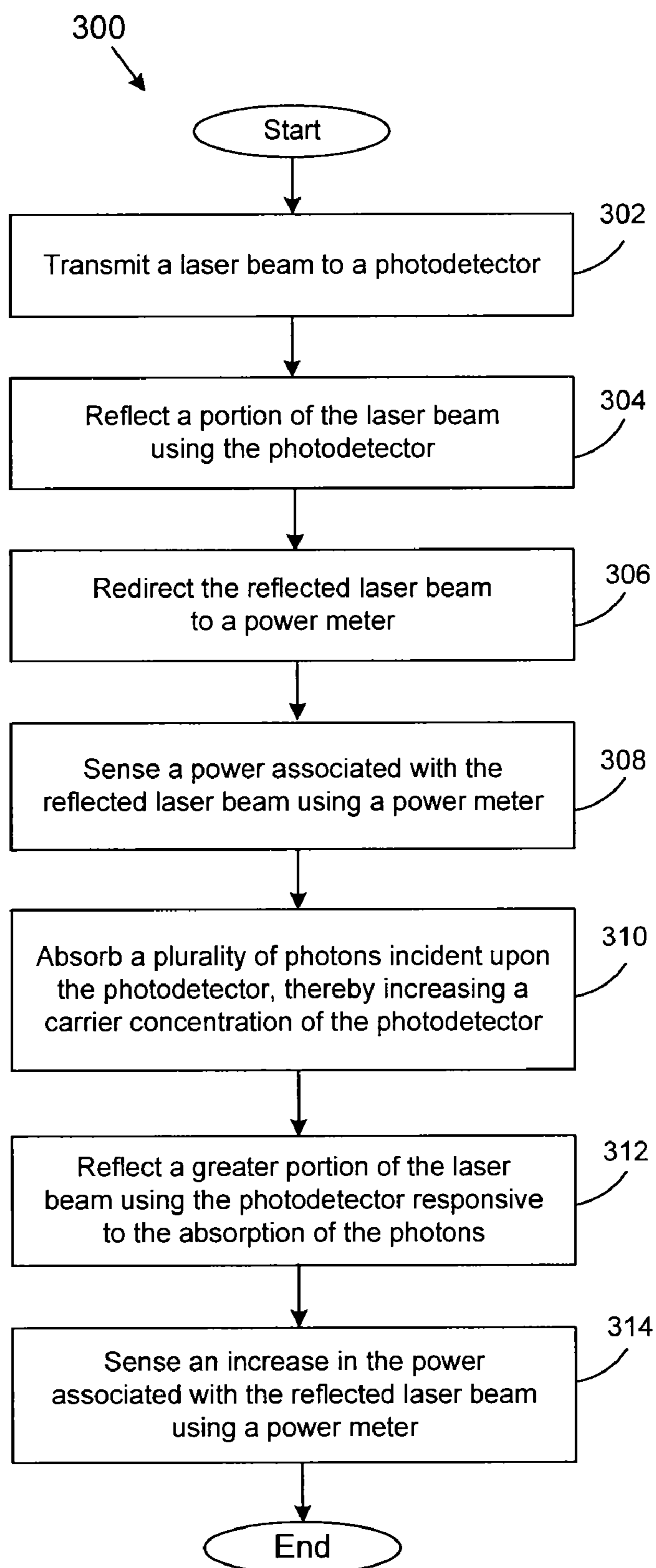
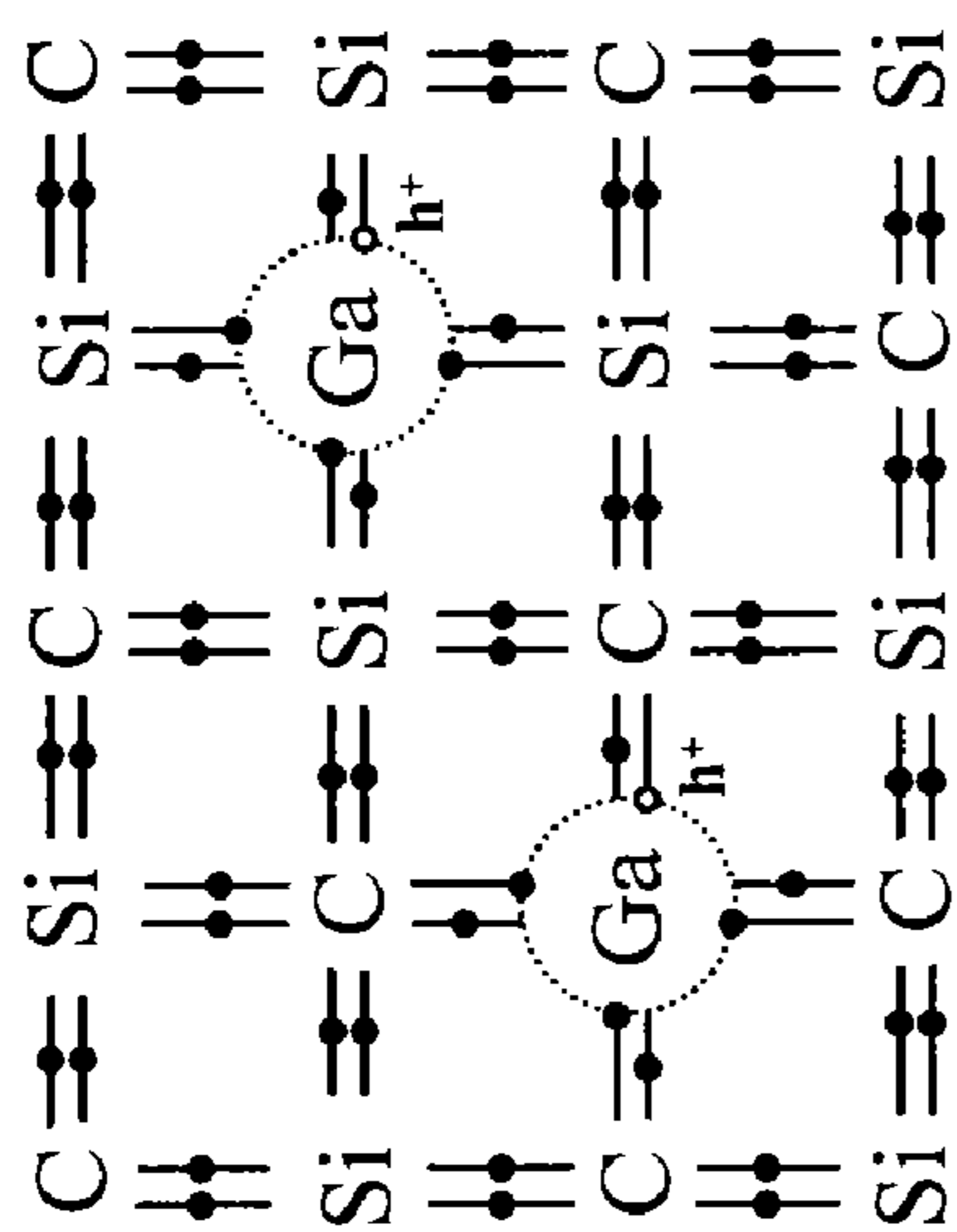
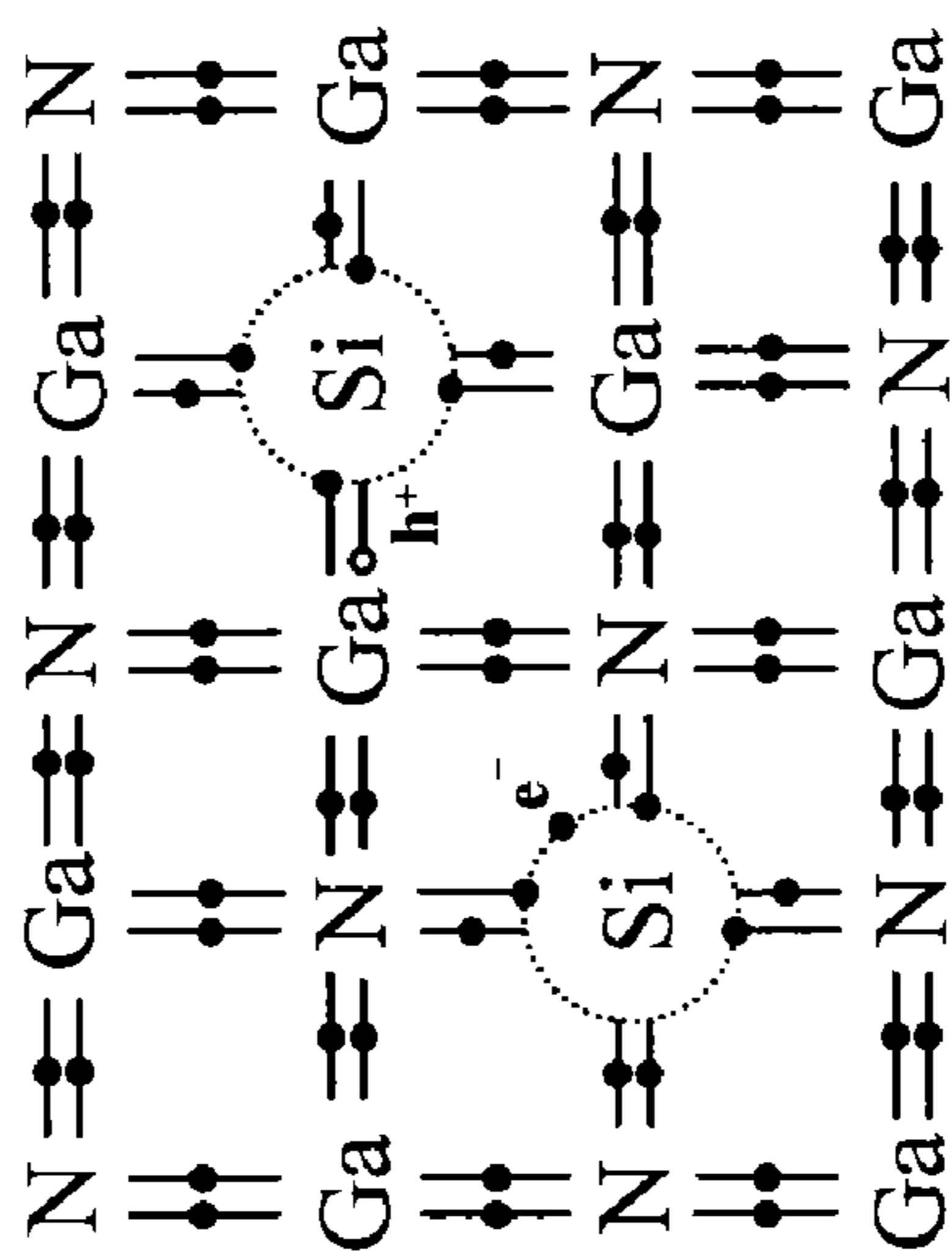


FIG. 2

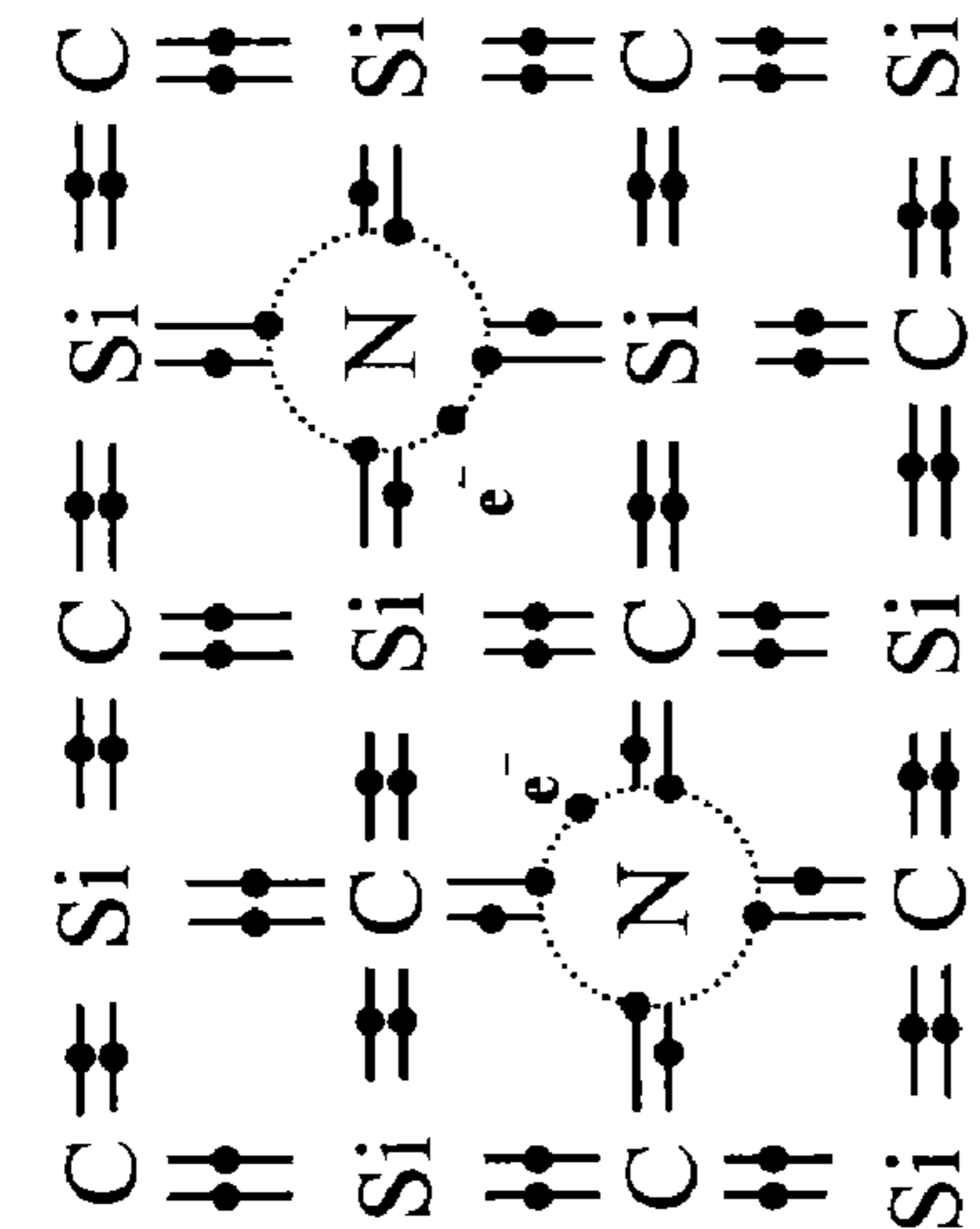
**FIG. 3**



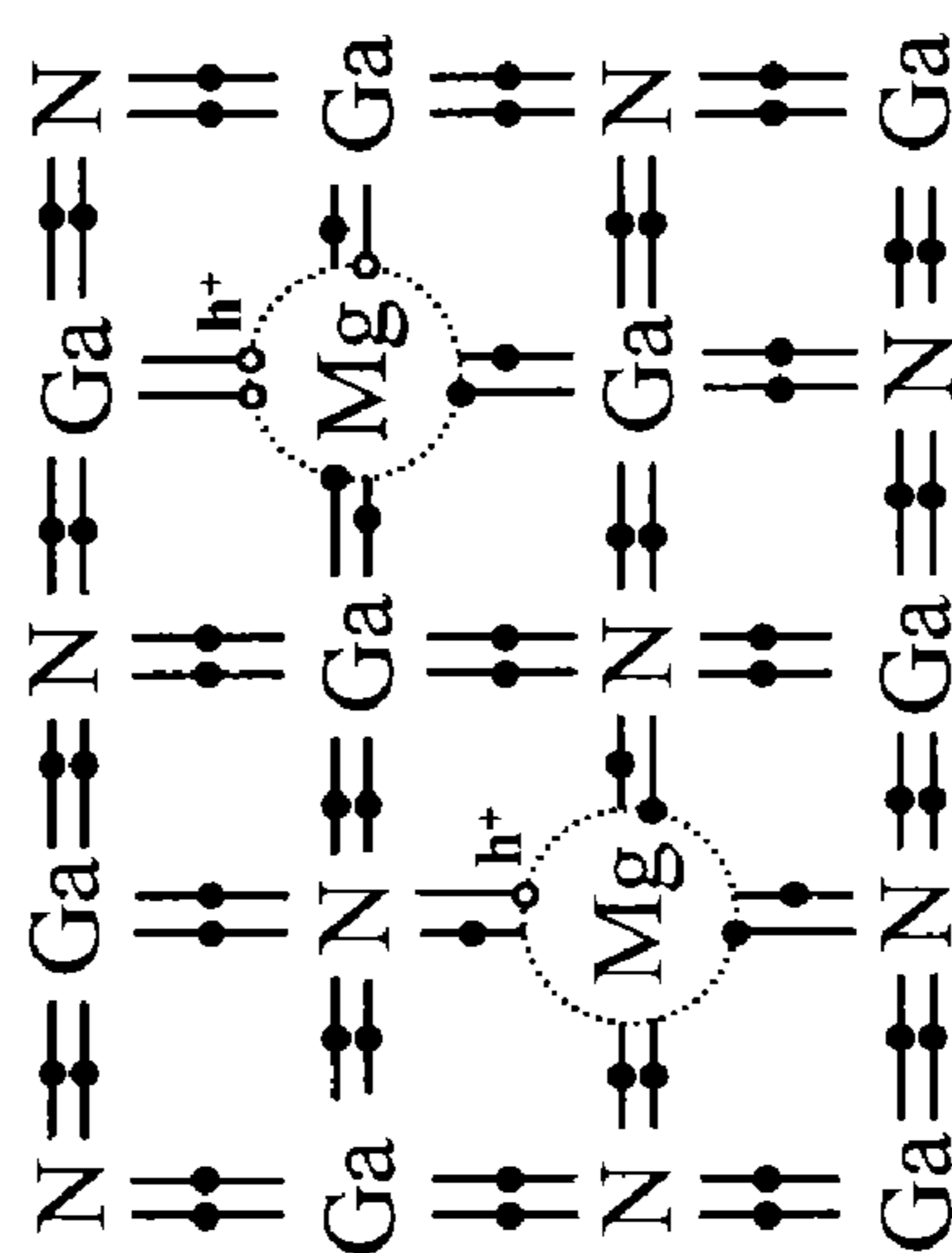
(A)



(B)



(C)



(D)

FIG. 4

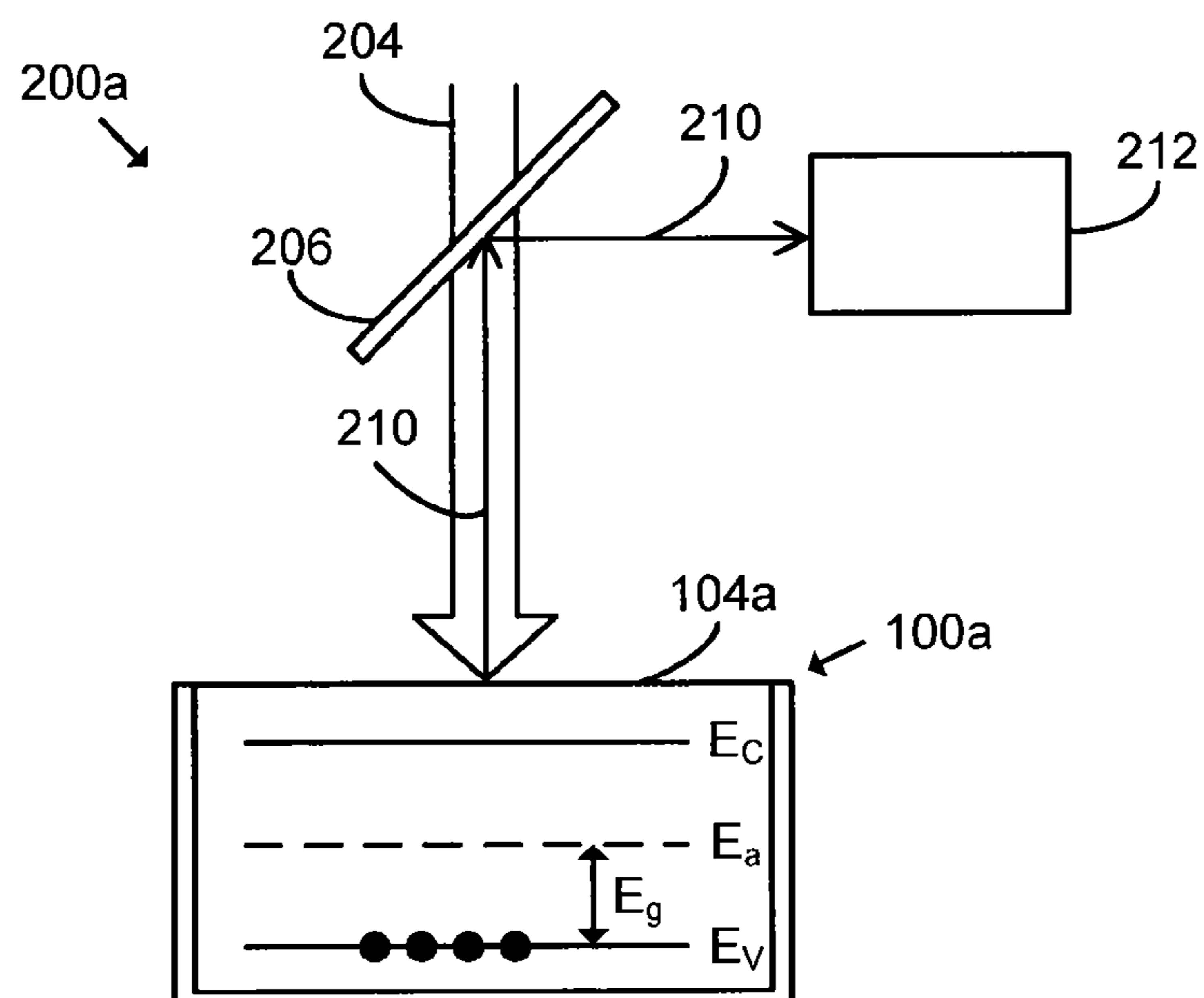


FIG. 5A

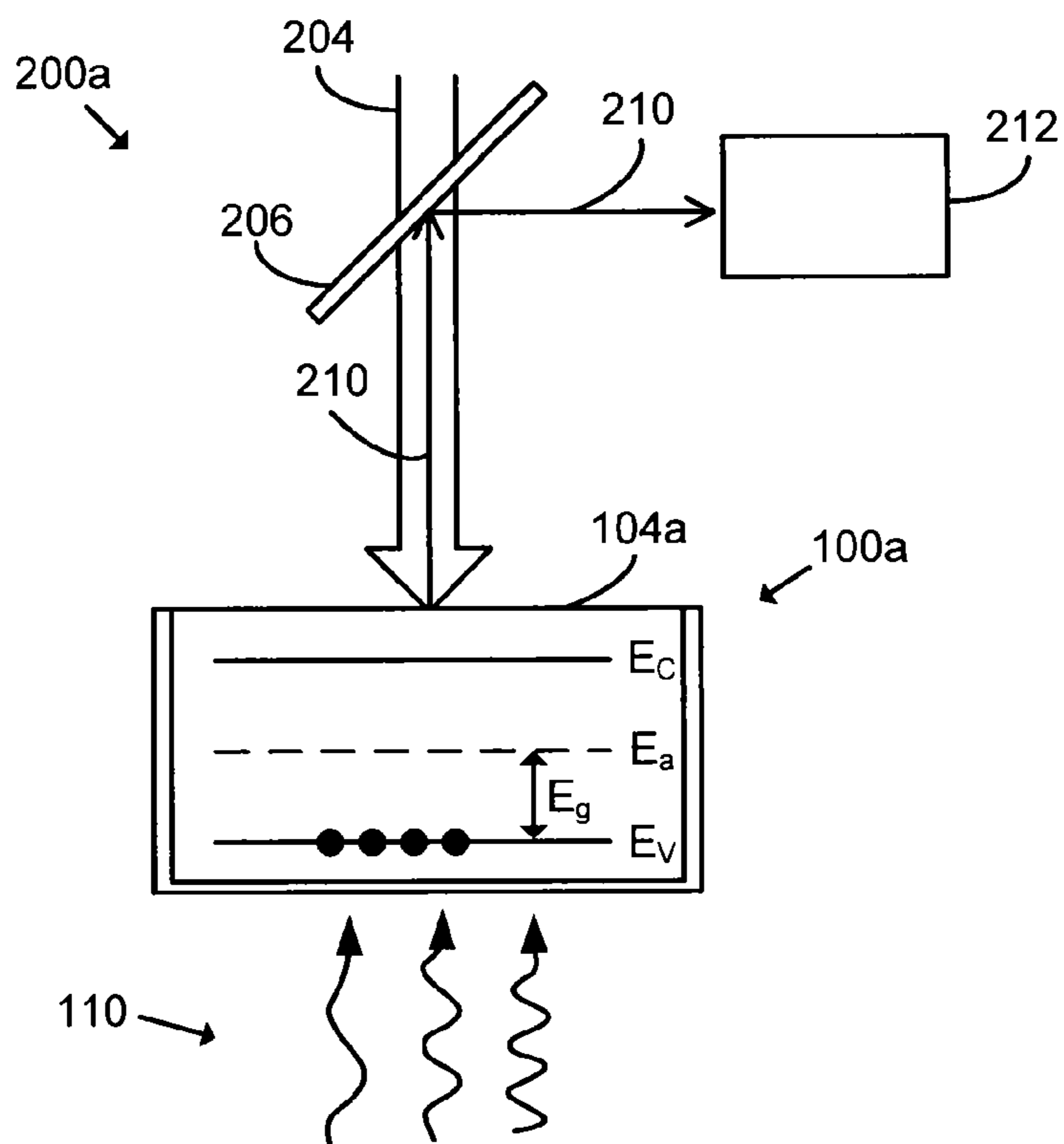


FIG. 5B

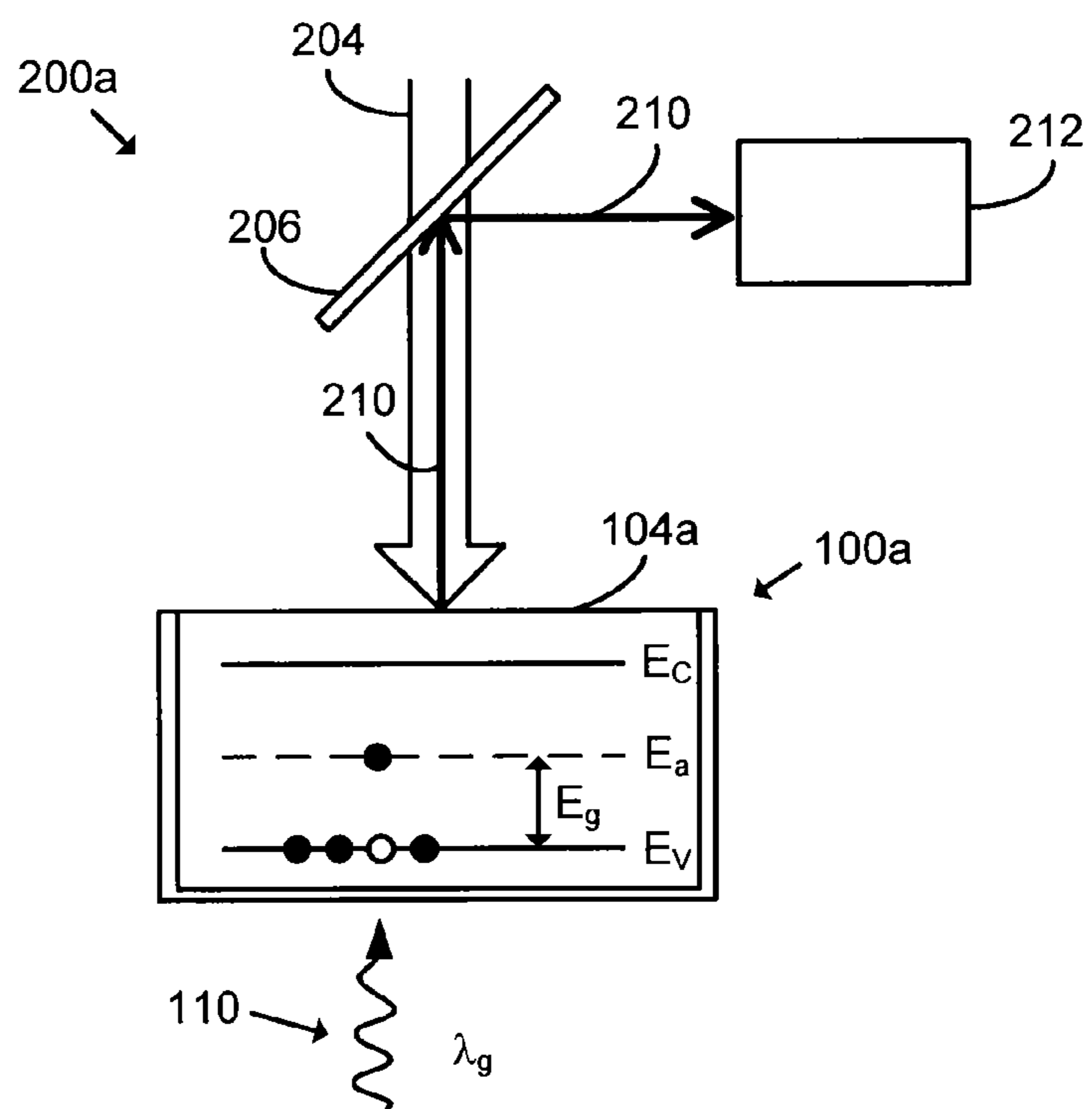


FIG. 5C

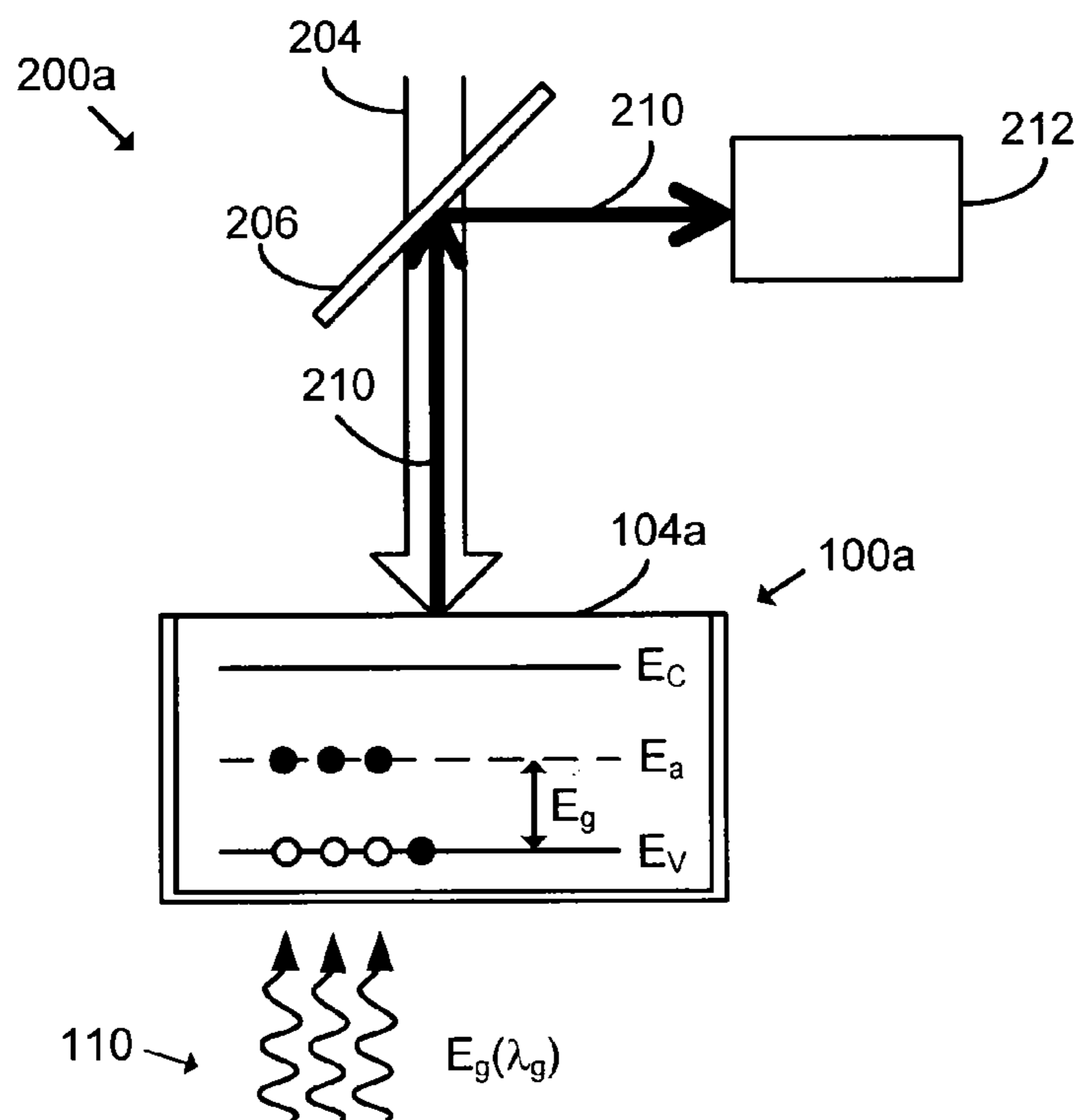


FIG. 5D

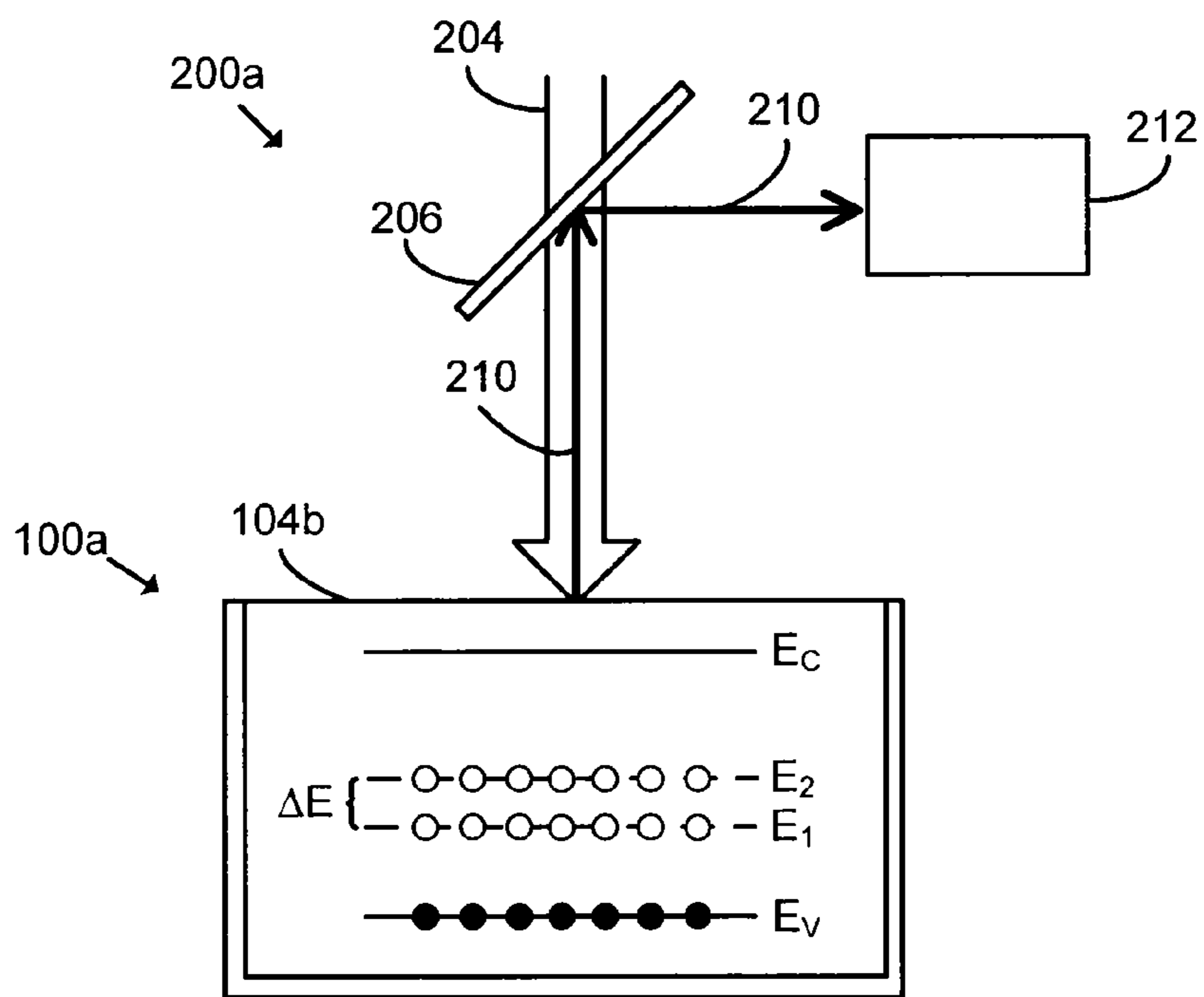


FIG. 6A

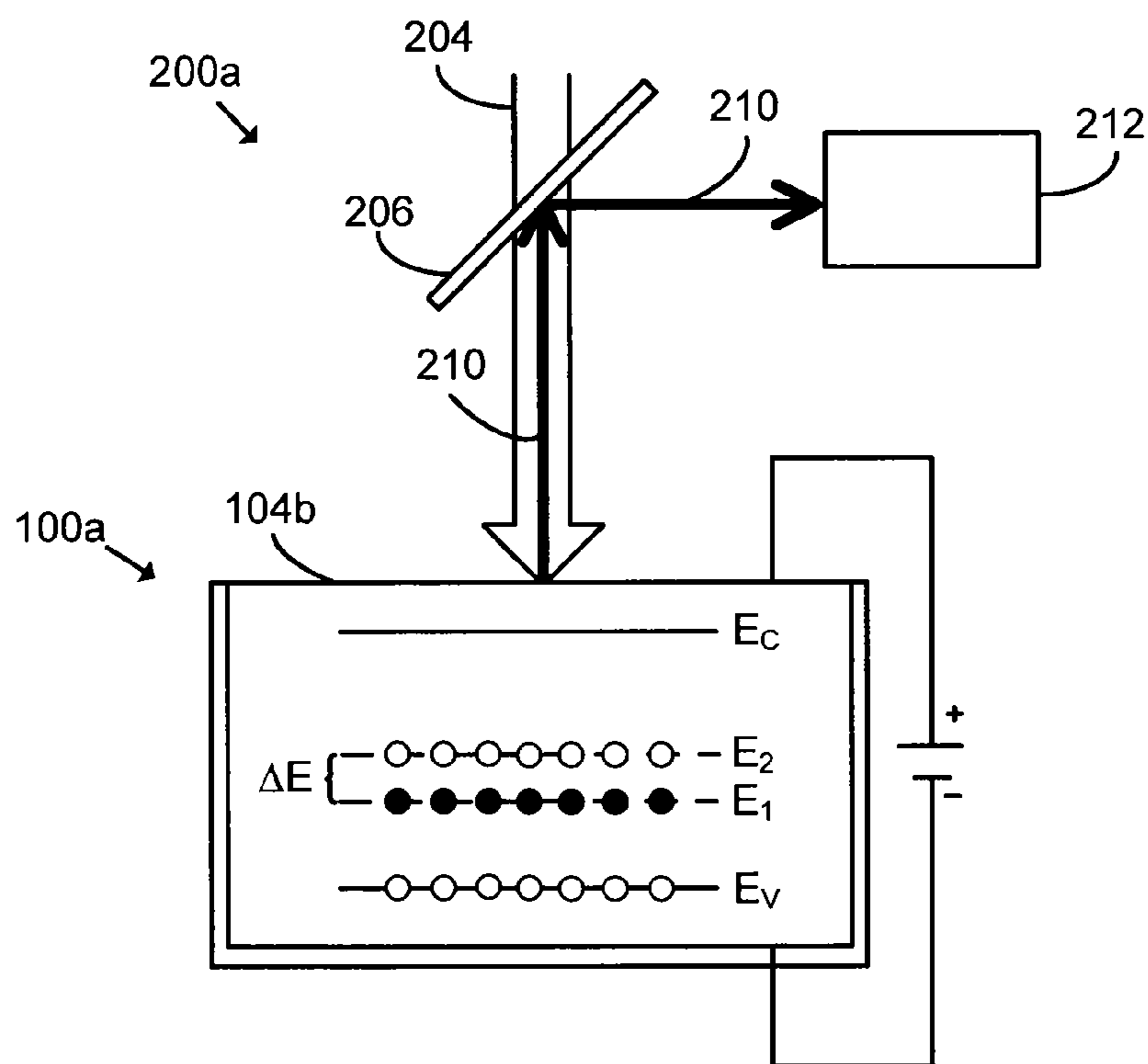


FIG. 6B

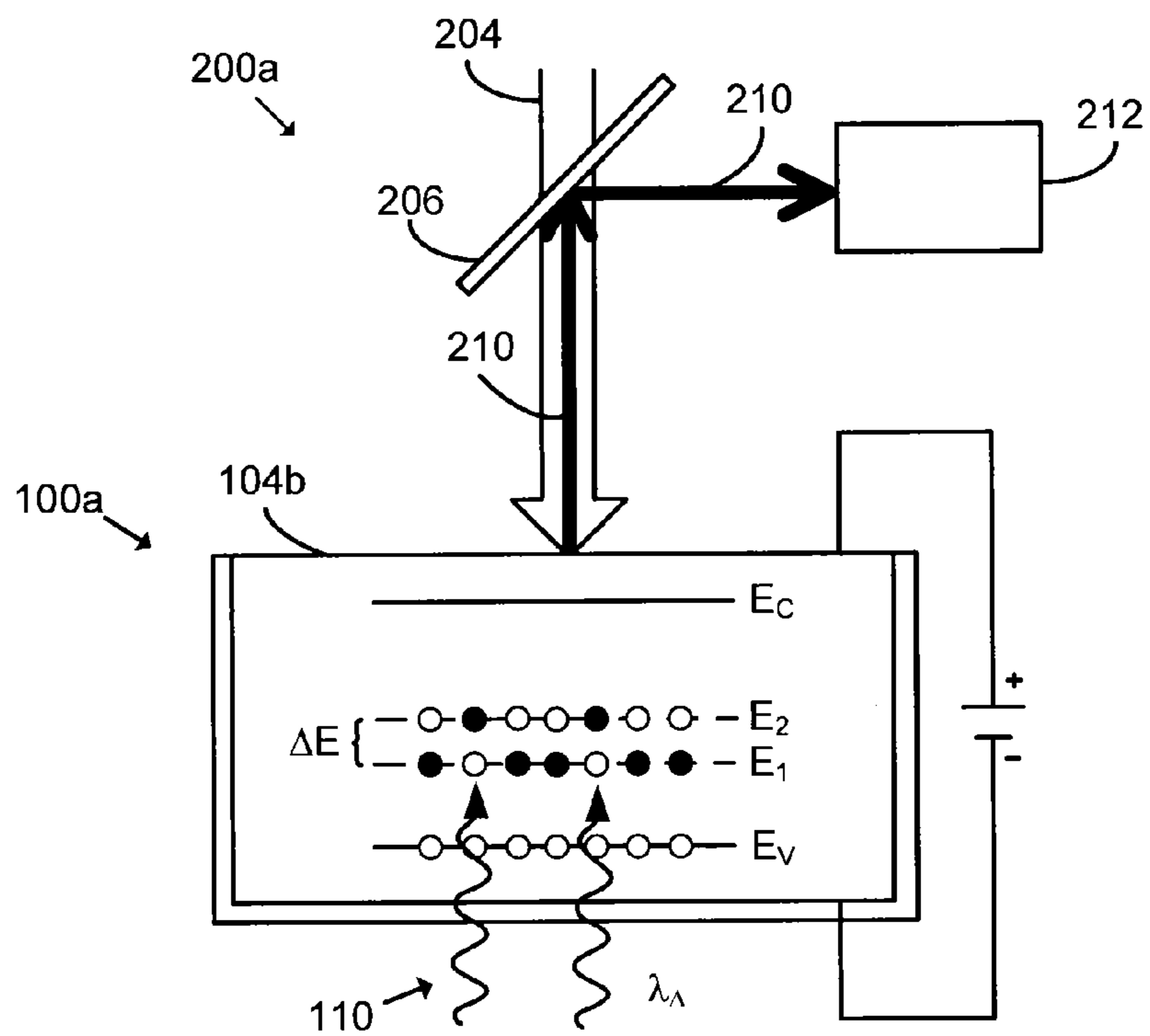


FIG. 6C

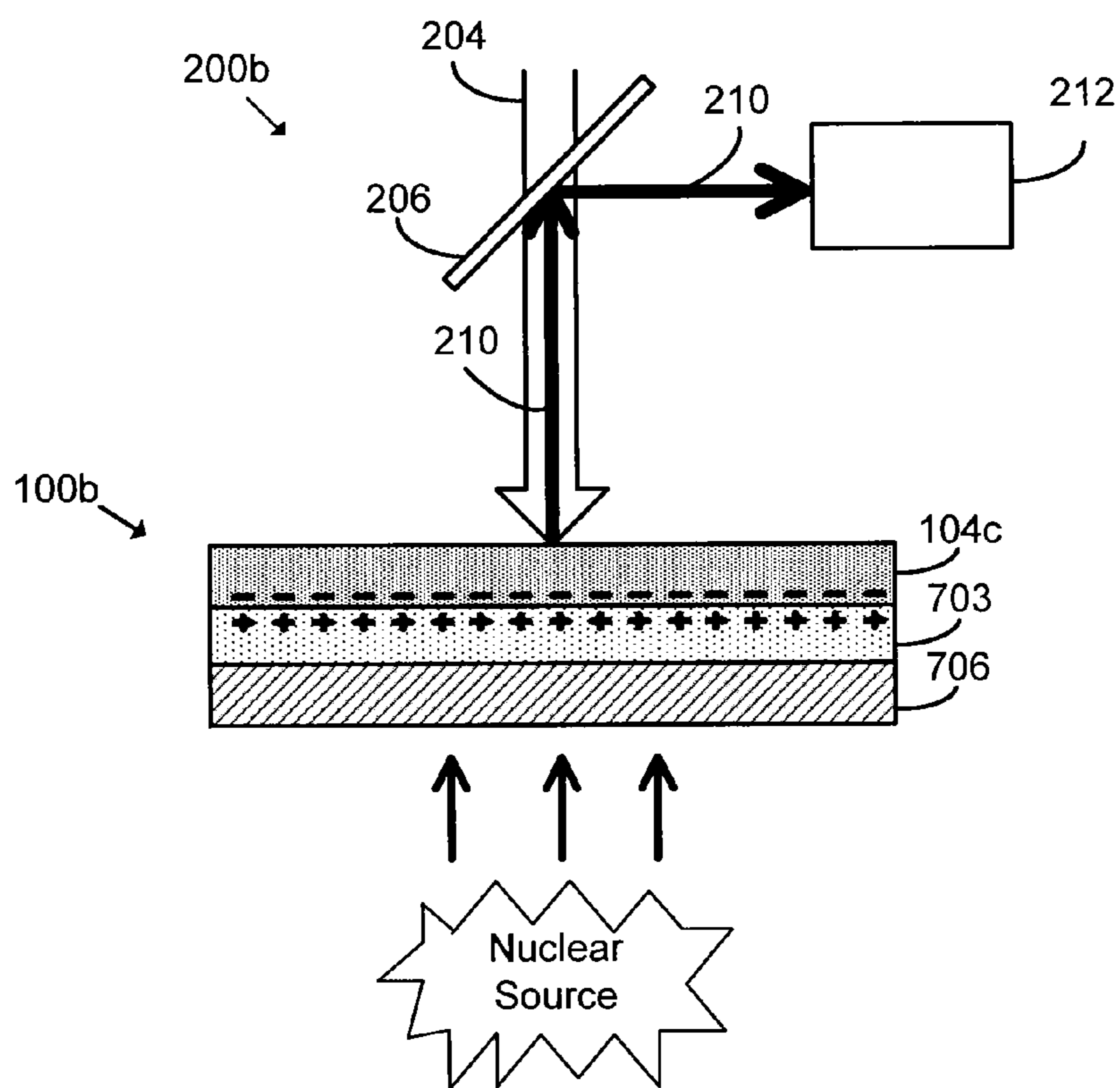


FIG. 7

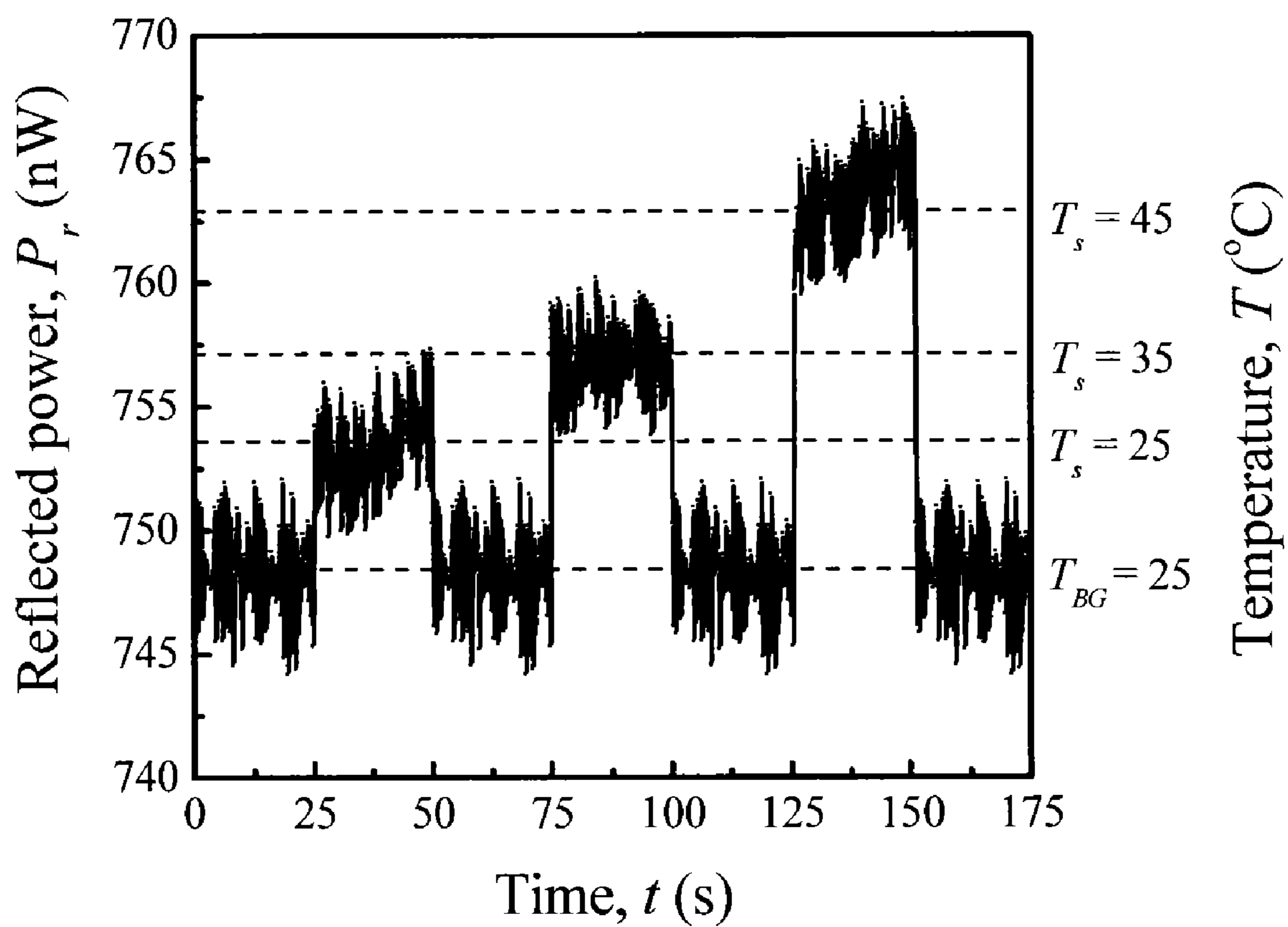


FIG. 8

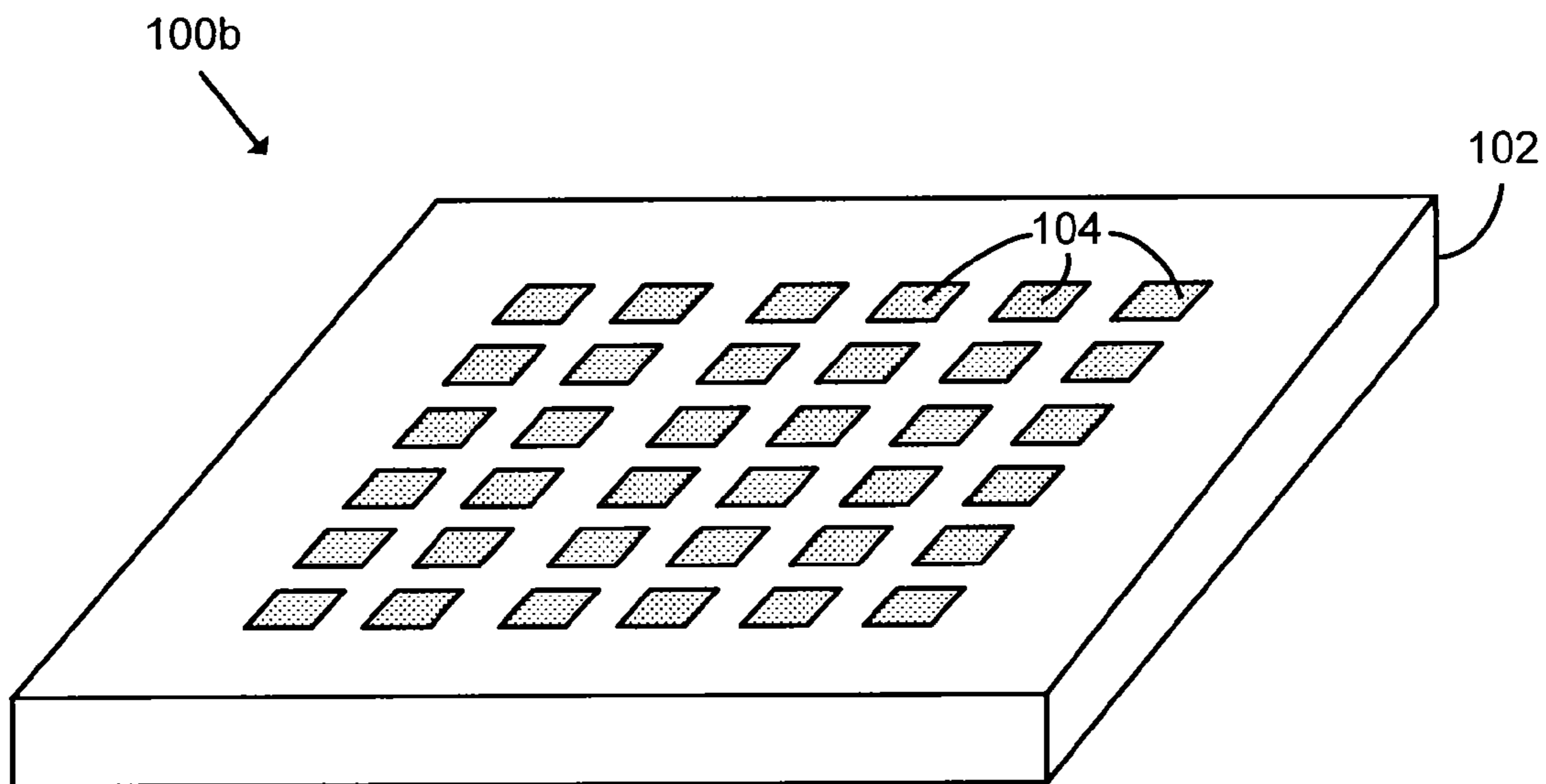


FIG. 9

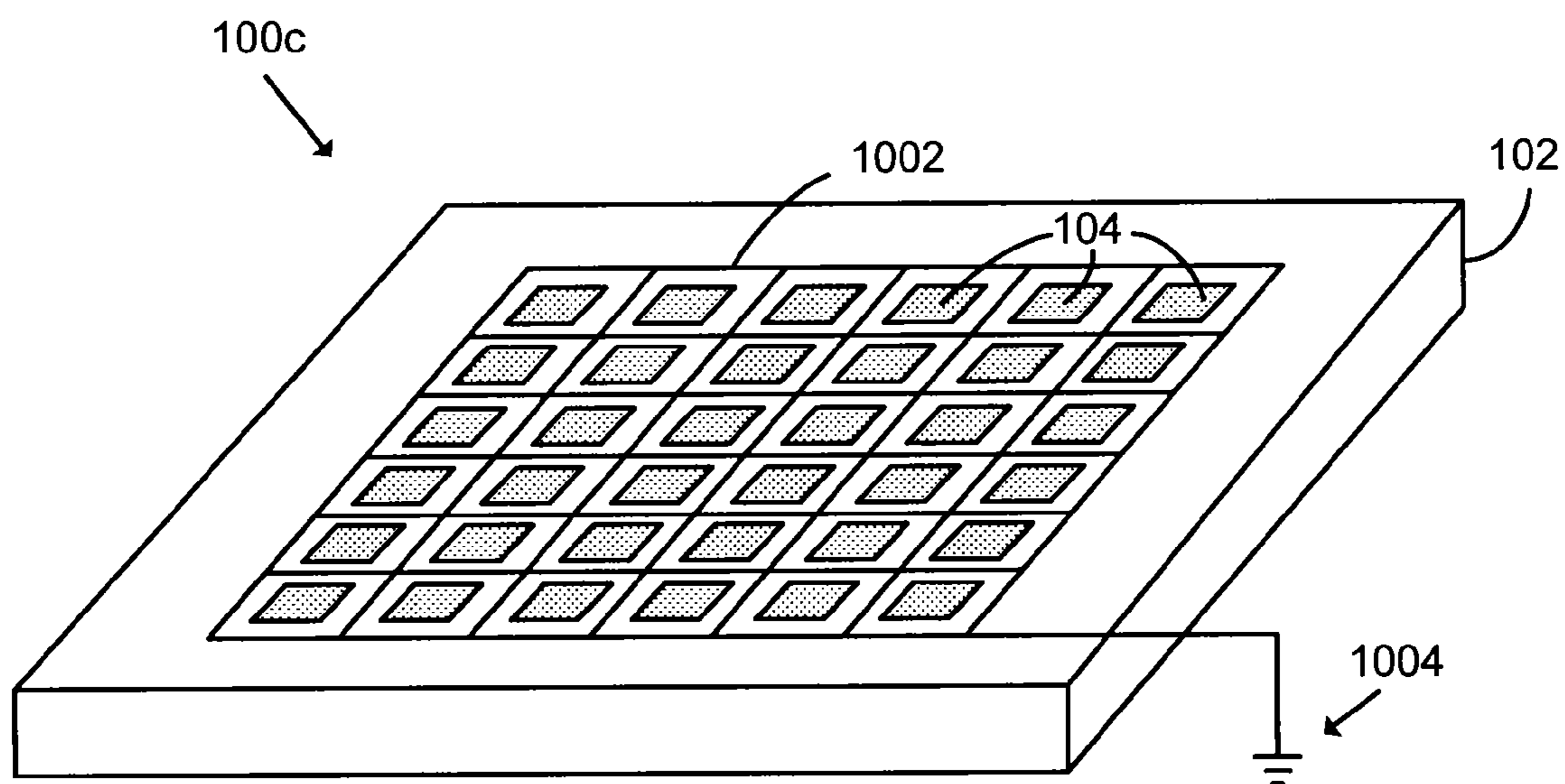


FIG. 10

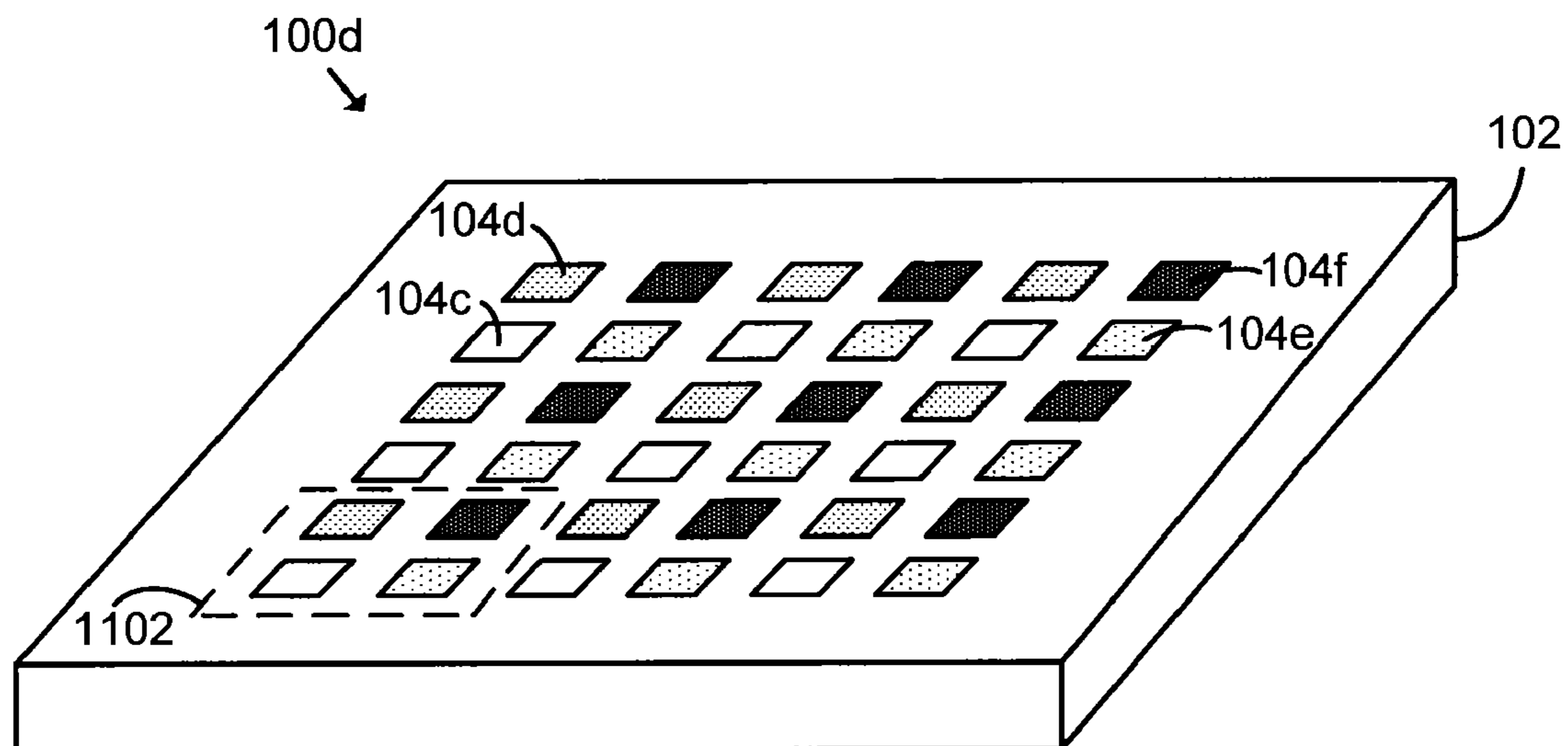


FIG. 11

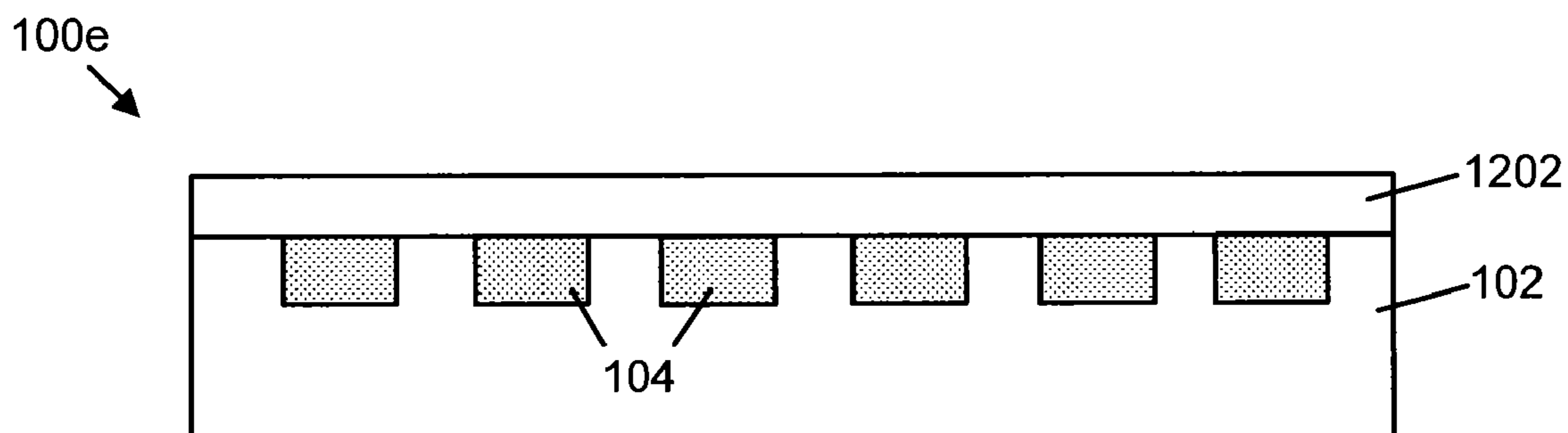


FIG. 12

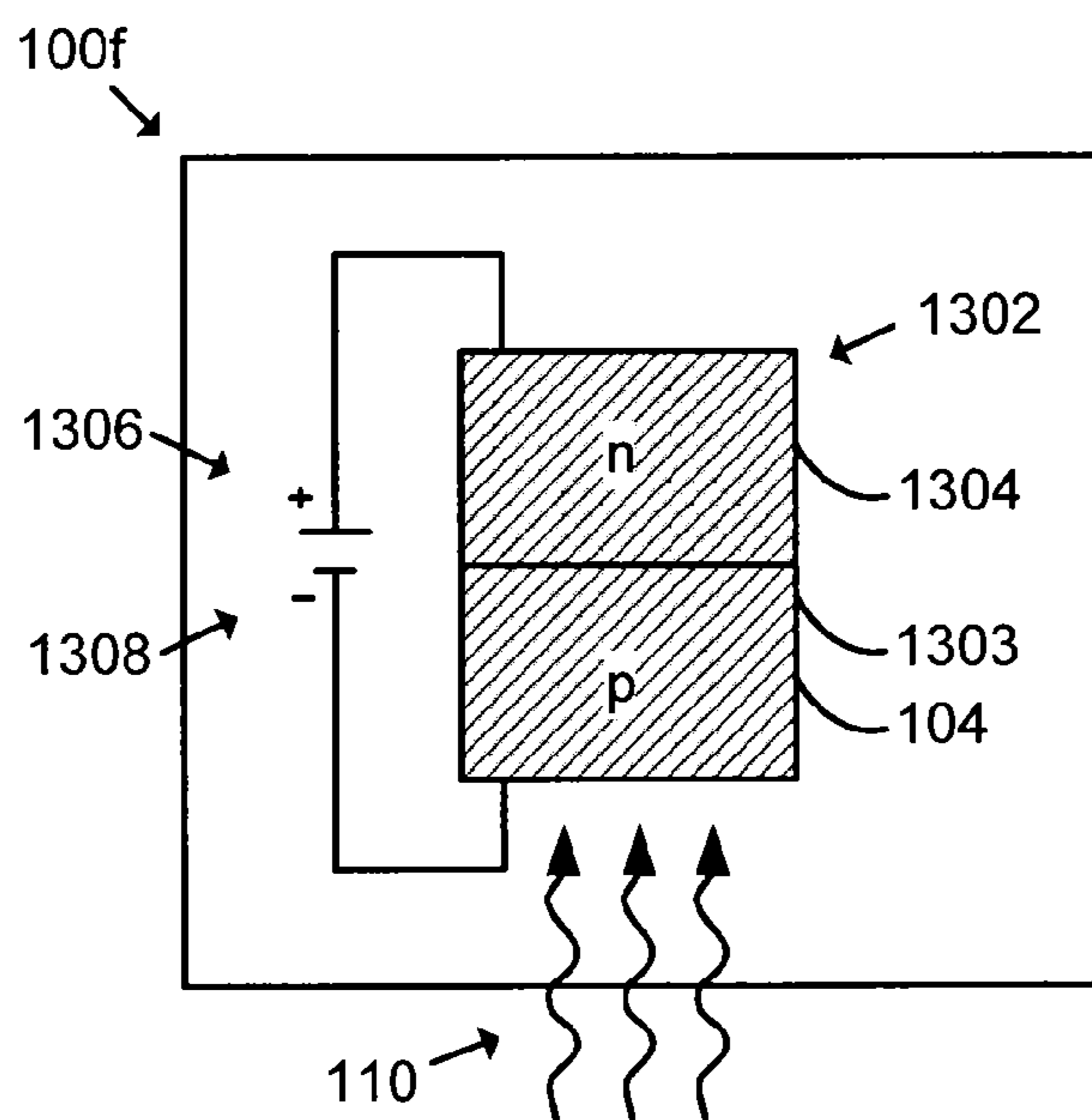


FIG. 13

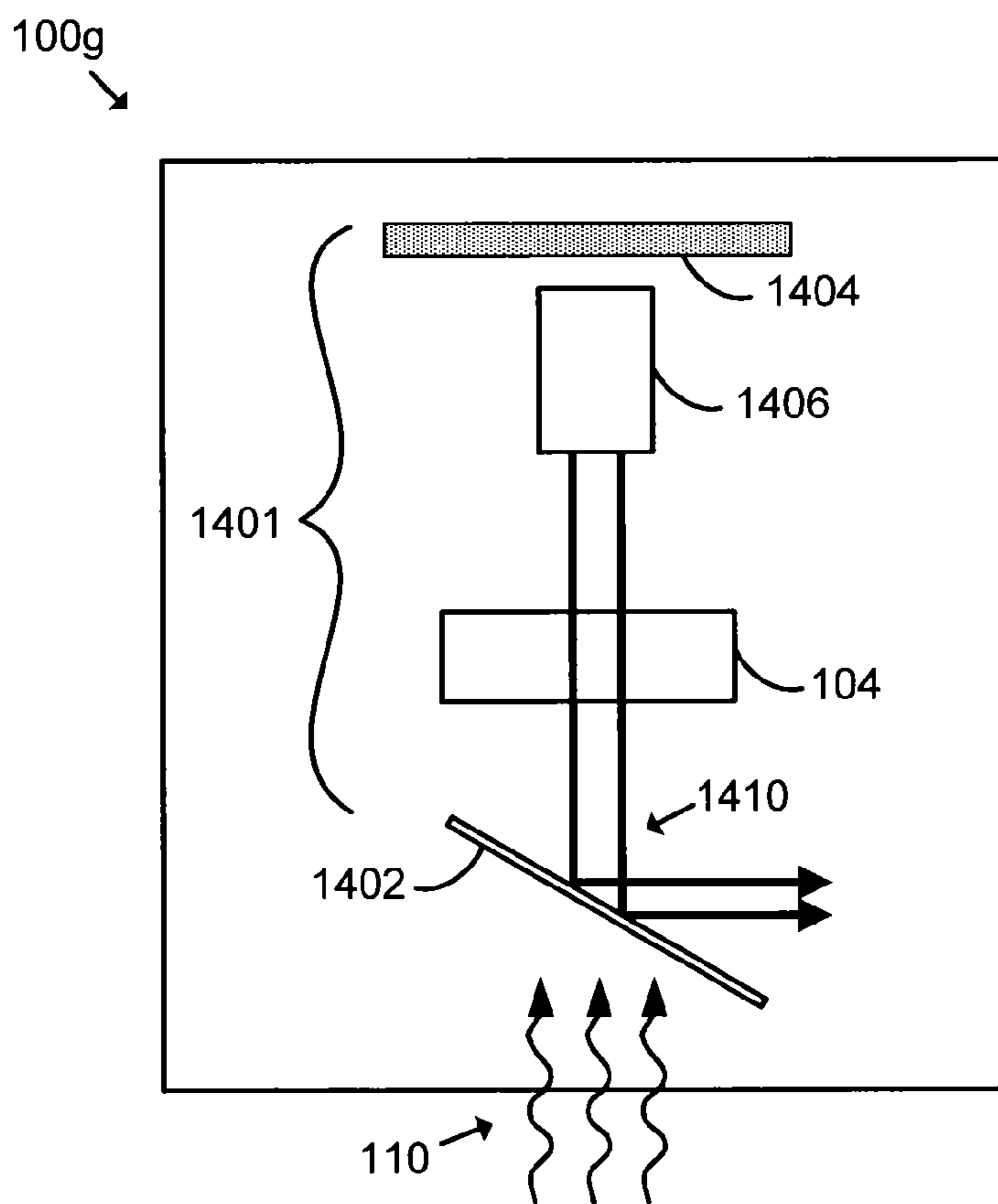


FIG. 14

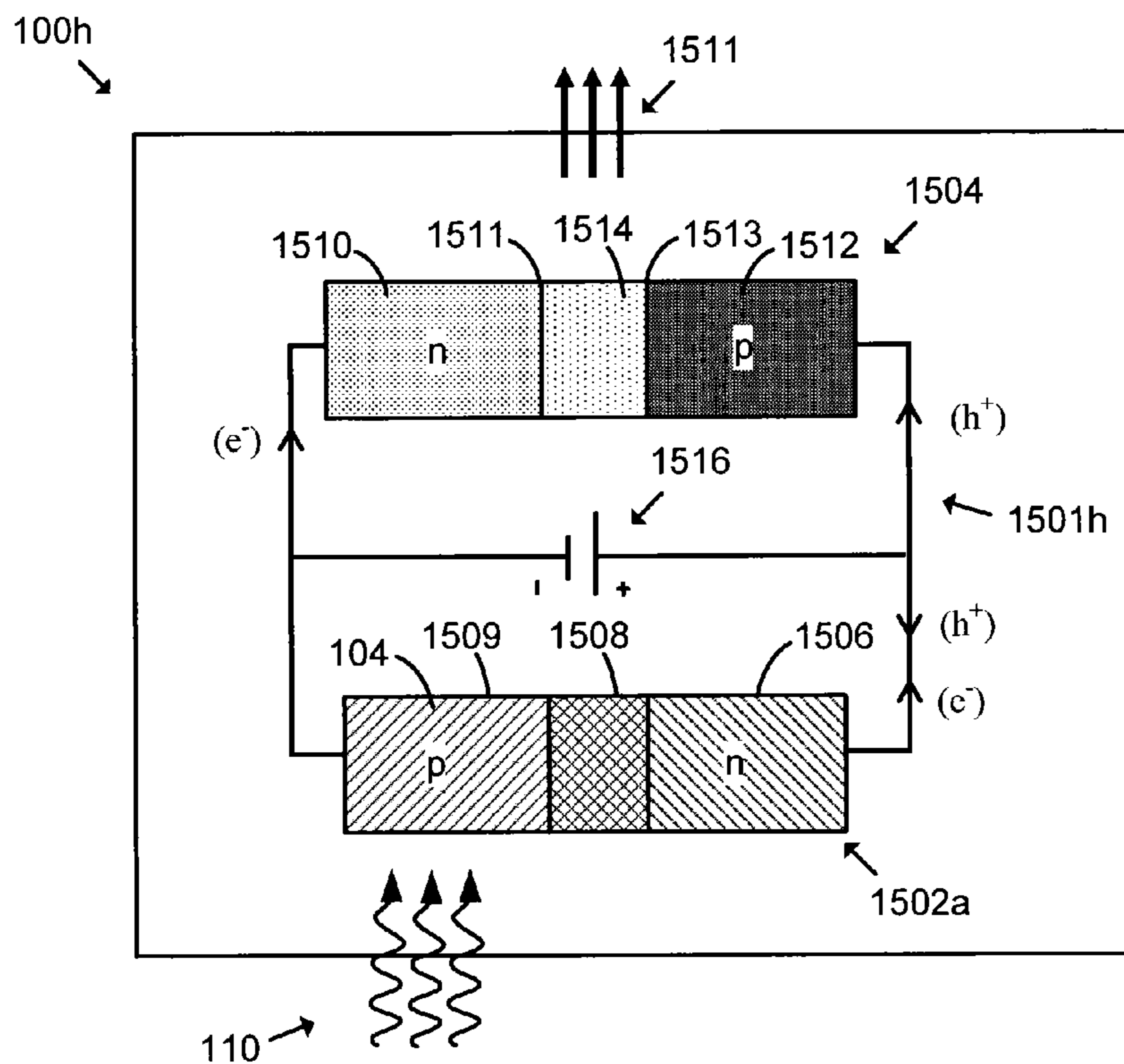


FIG. 15A

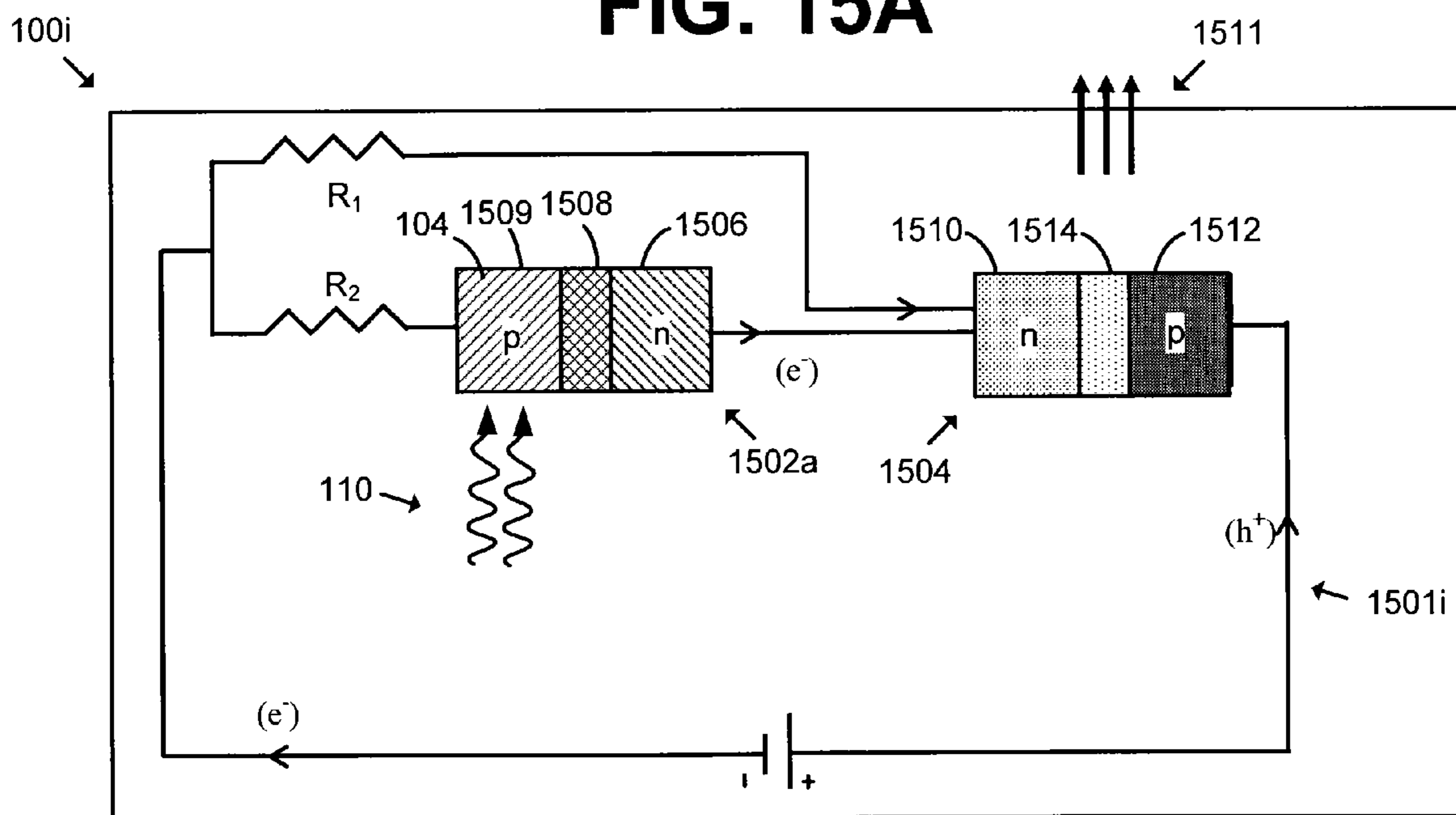


FIG. 15B

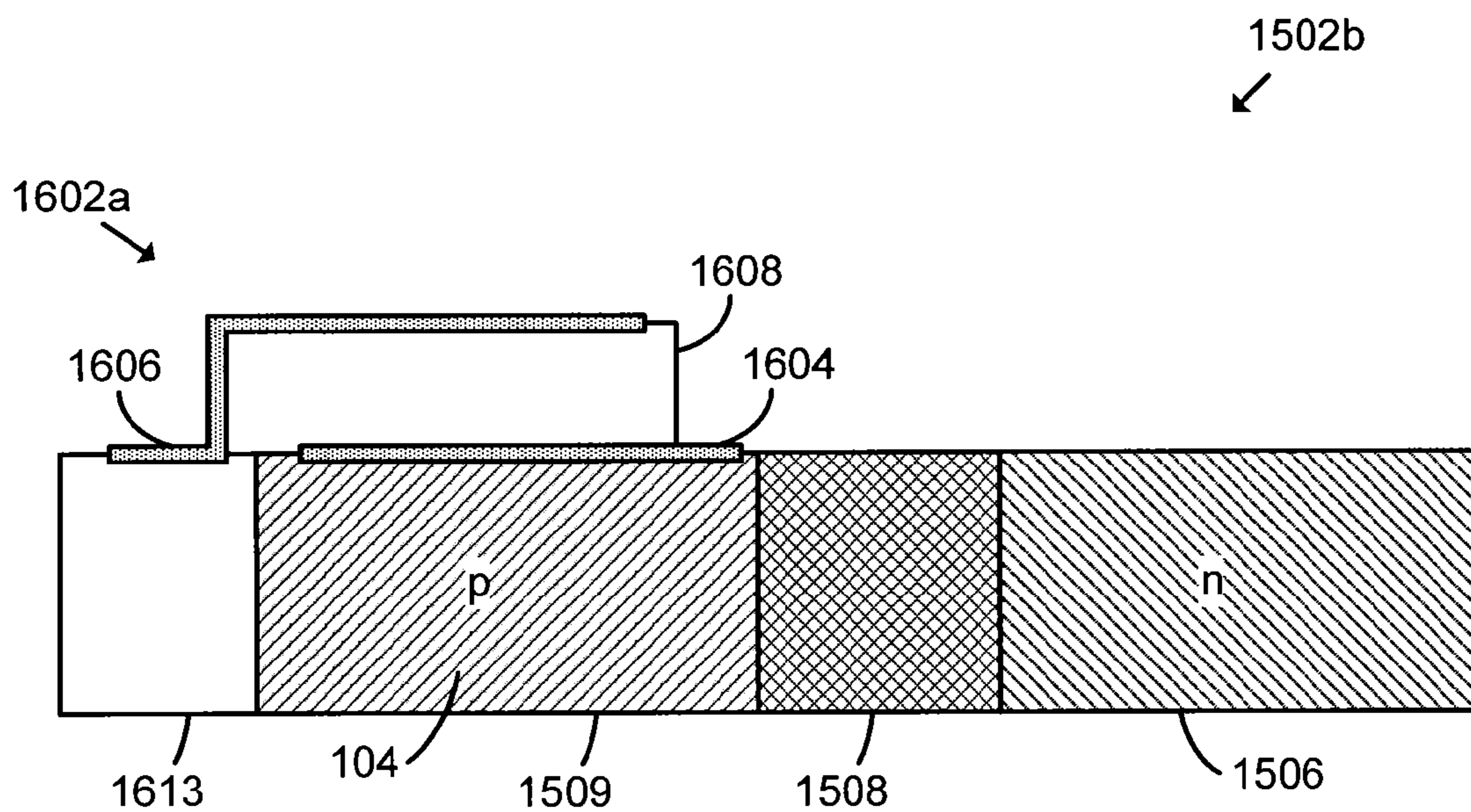


FIG. 16

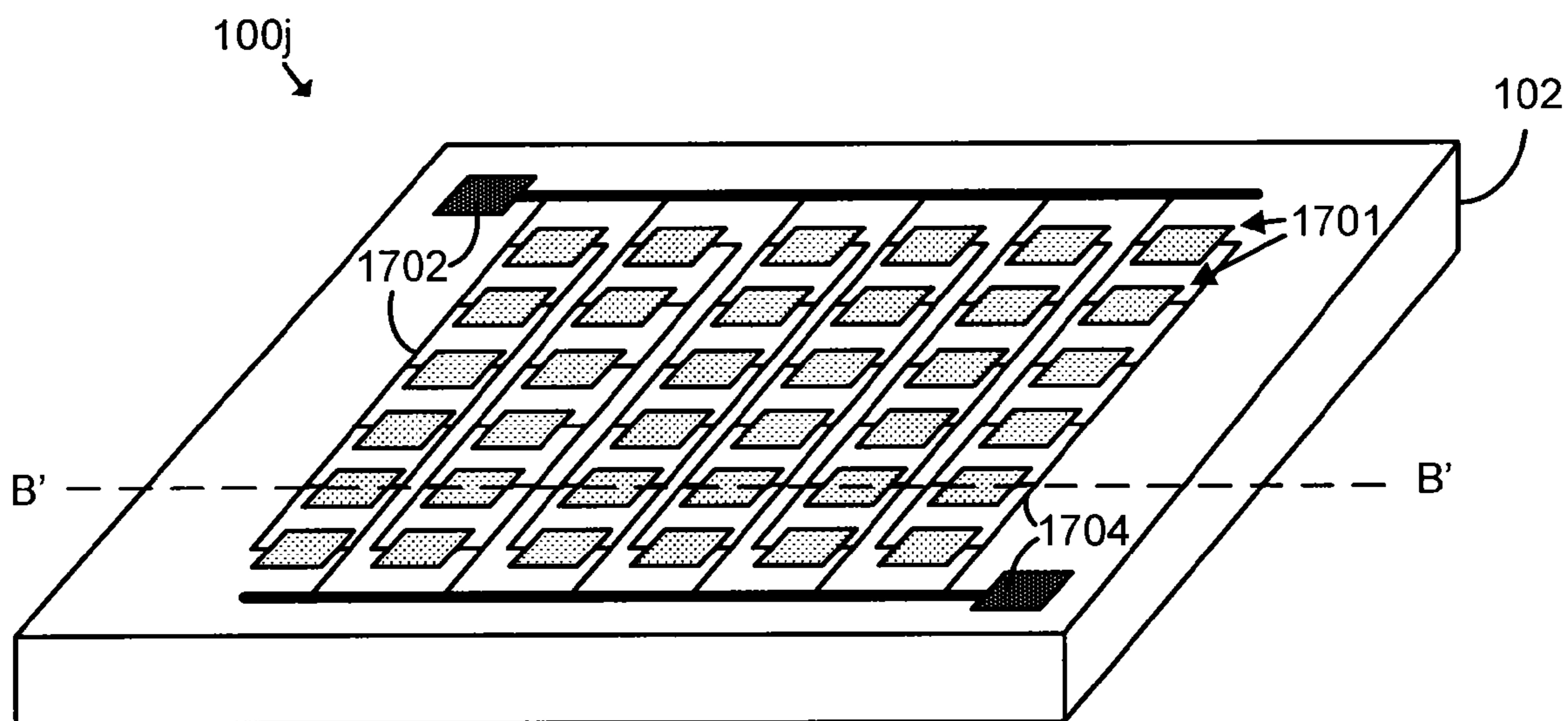


FIG. 17

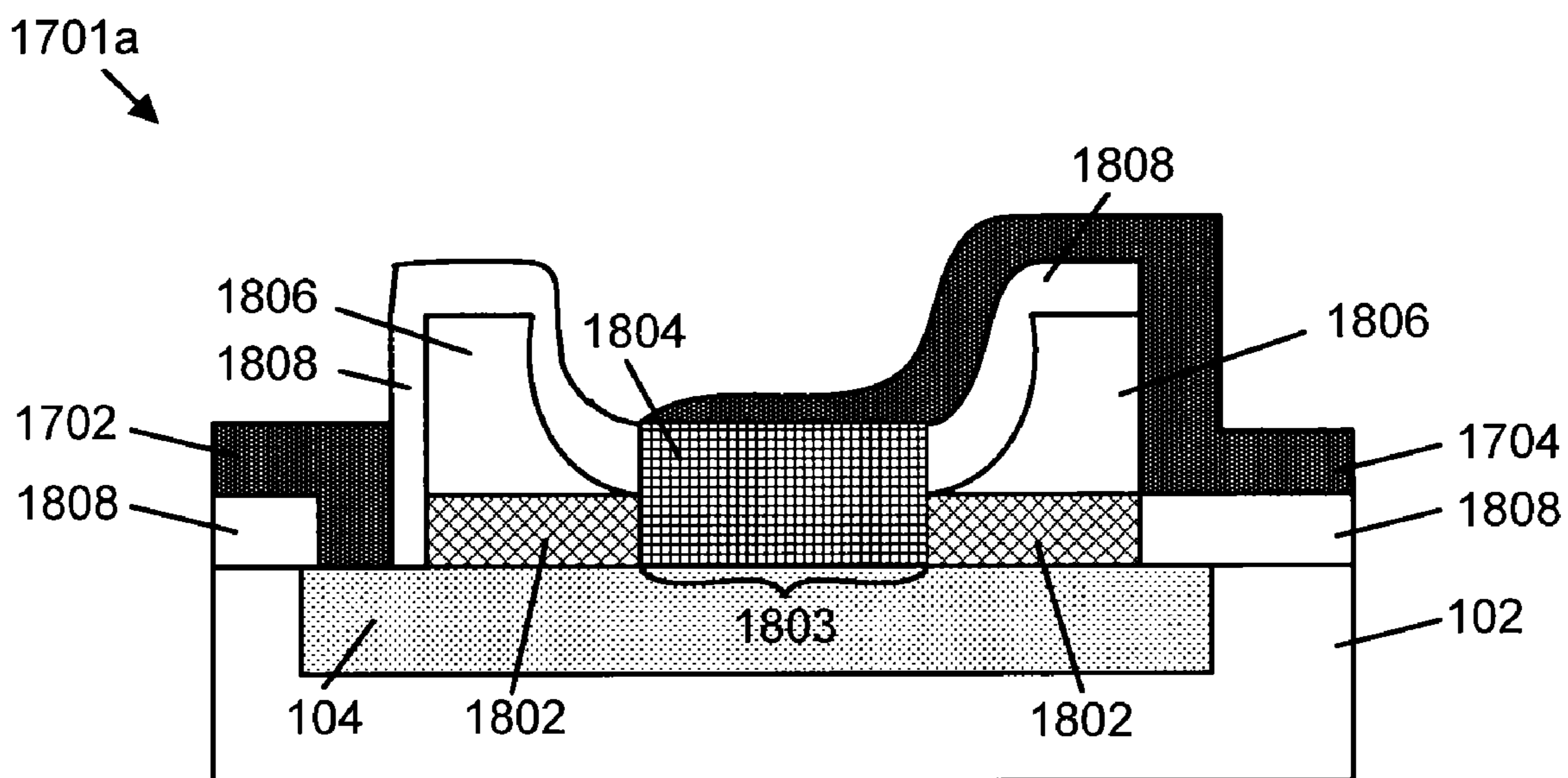


FIG. 18A

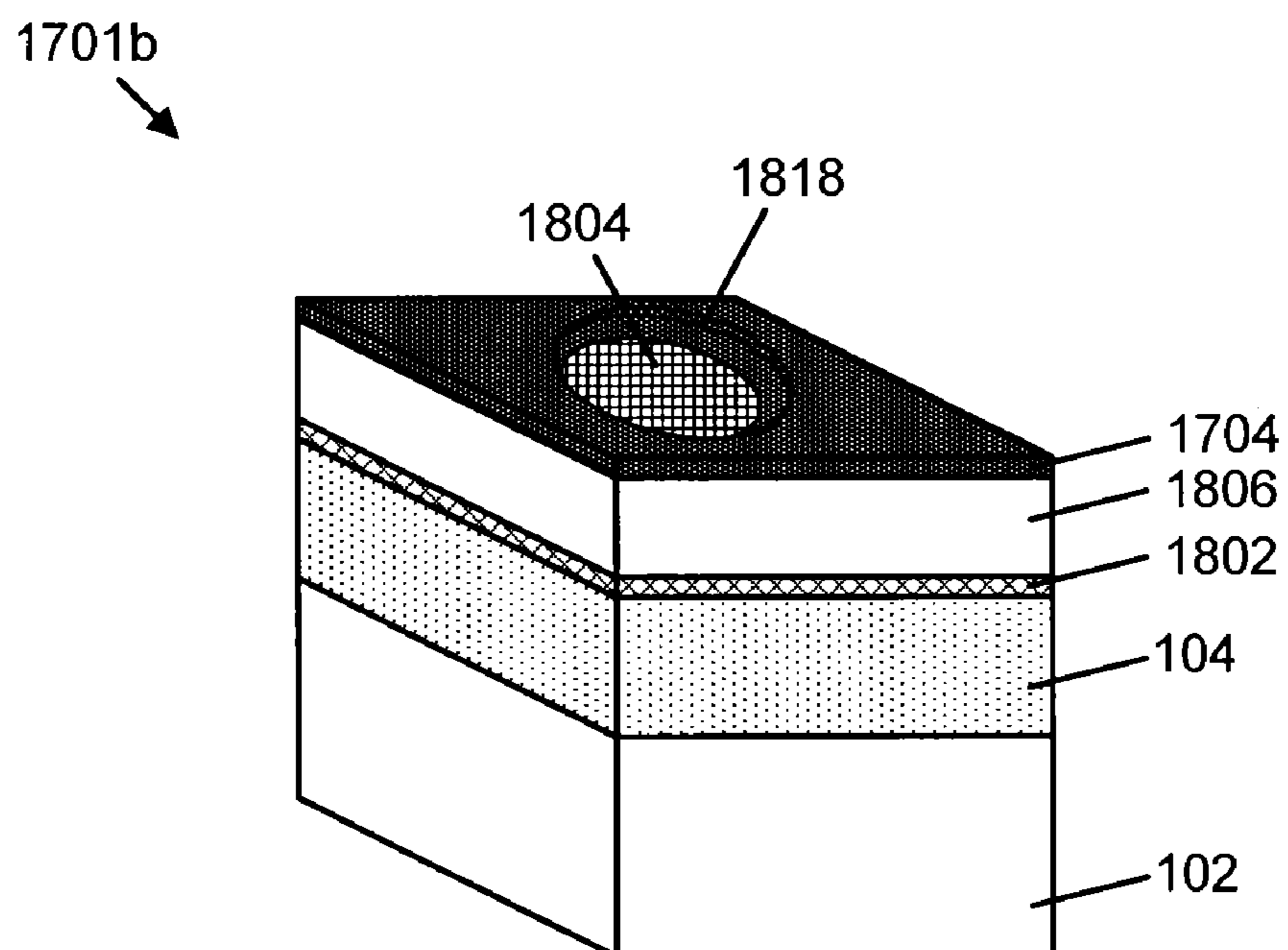


FIG. 18B

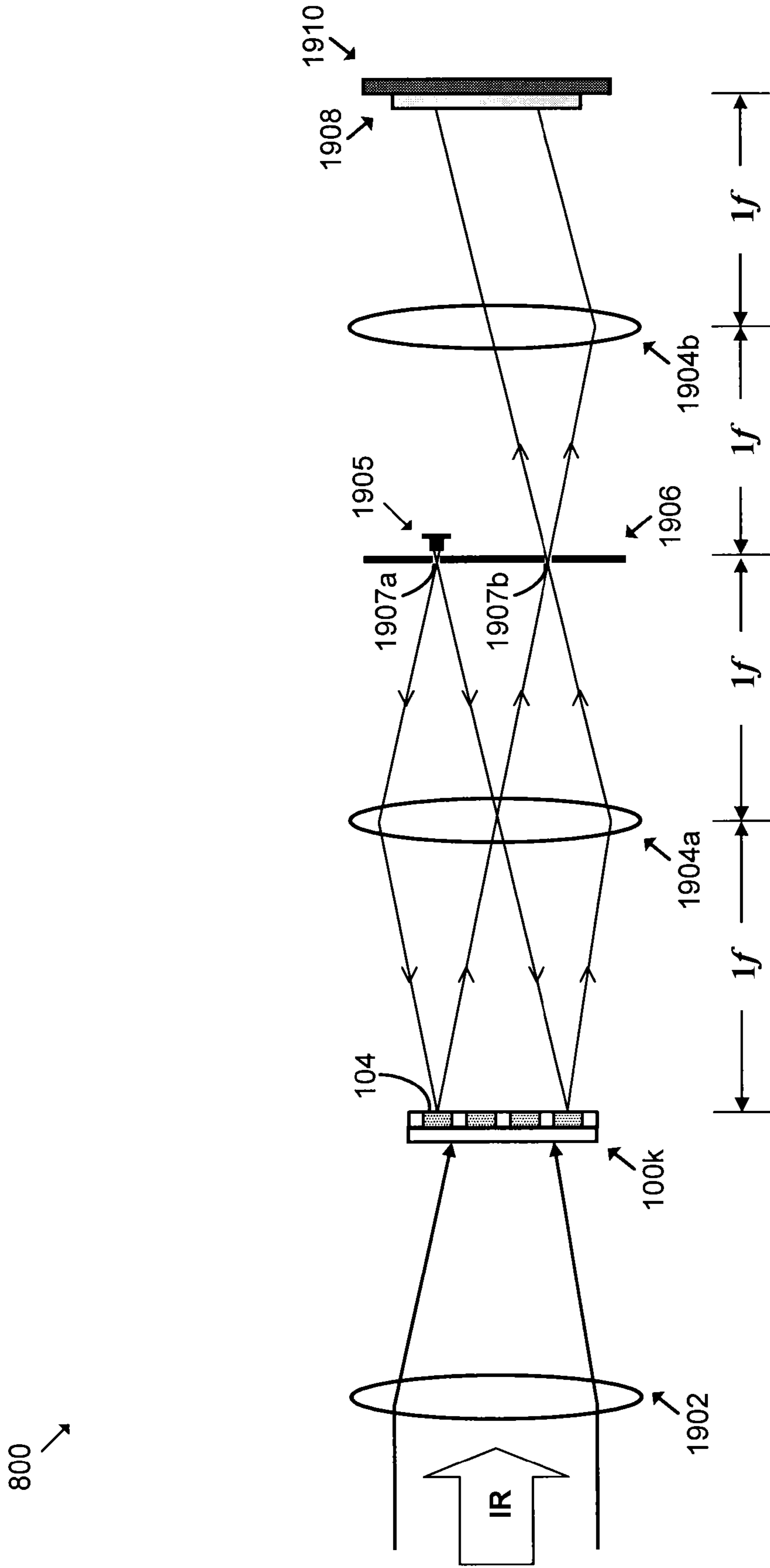


FIG. 19

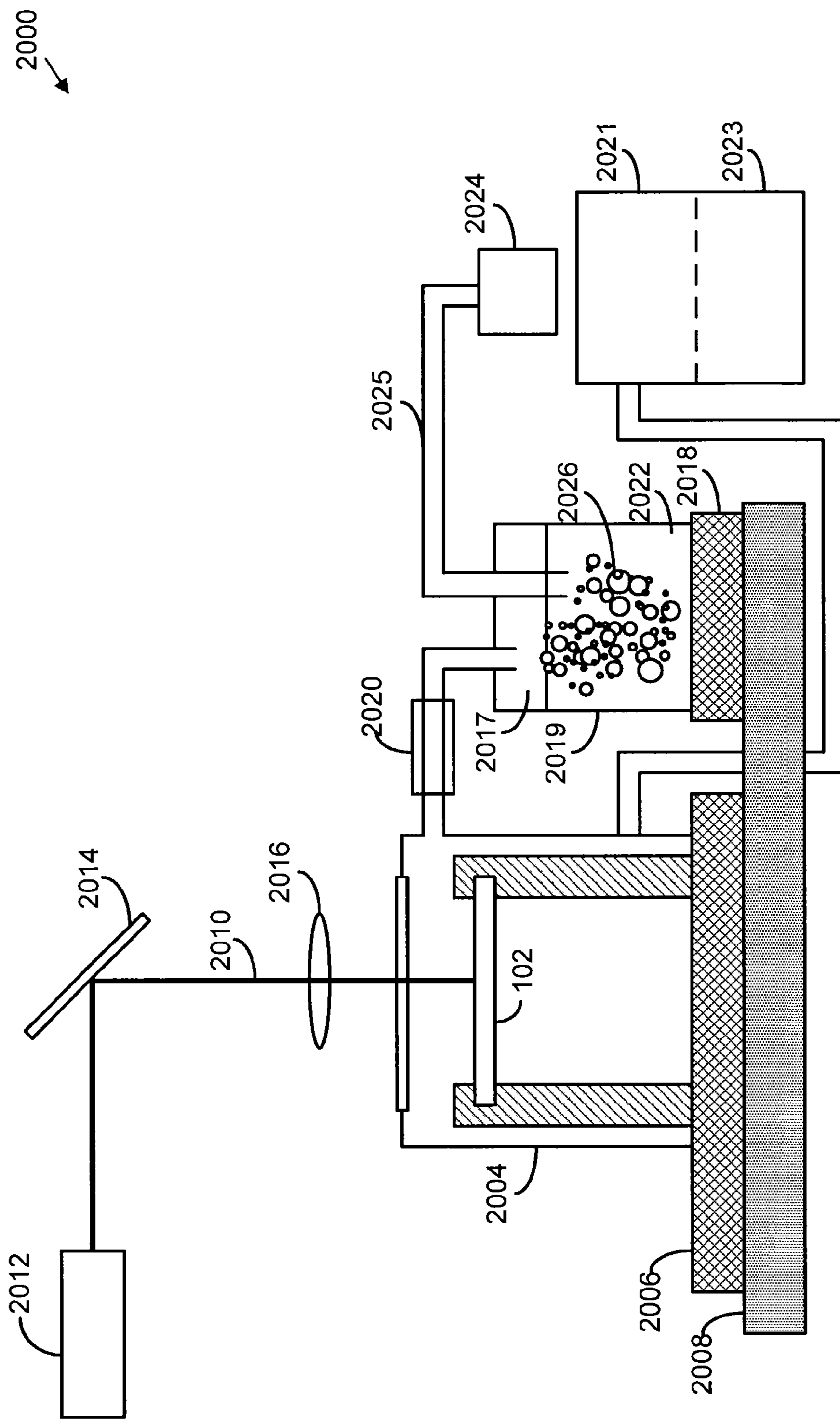
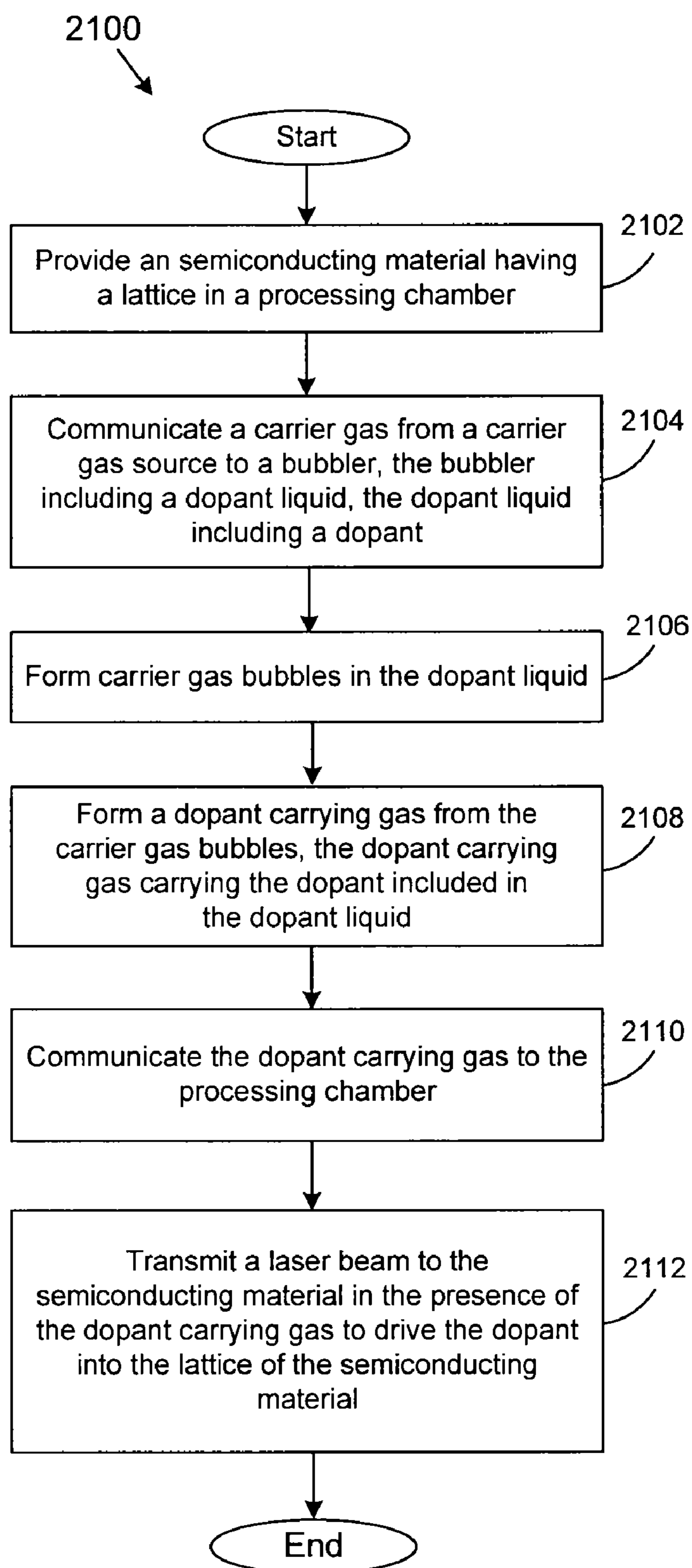


FIG. 20

**FIG. 21**

PHOTODETECTION

CROSS-REFERENCE TO RELATED APPLICATION

[0001] This application claims priority to copending U.S. Provisional Application entitled, "Frequency-Tuned Detectors Coupled with Optical Amplifiers for Weak Signal Detection," having Ser. No. 61/378,498, filed Aug. 31, 2010, which is incorporated herein by reference in its entirety.

STATEMENT REGARDING FEDERALLY SPONSORED RESEARCH

[0002] This disclosure was made with United States Government support under Contract Number N66604-09-M-3087 awarded by the Naval Undersea Warfare Center. The United States Government has certain rights in any patent that issues from the present application.

TECHNICAL FIELD

[0003] The present disclosure is generally related to sensors and, more particularly, is related to detection of photons.

BACKGROUND

[0004] In general, remote sensing technologies use one of the following techniques: a) a battery-powered sensor/detector and transmitter, b) a remotely radio-frequency (RF) powered sensor/detector and transmitter, and c) a wave guide-delivered optical signal that produces a reflected signal back to a sensor/detector where the signal can be used for analysis. The latter technique is often used in one of two ways. The first method is where the optical signal is used in conjunction with a fiber optic wave guide where changes in the index of refraction of the waveguide can be used to determine environmental factors such as temperature of fiber or the mechanical force being applied to the fiber. The second approach requires the fiber to collect a light from the radiation source and/or reflected signal from the fiber and deliver the captured light back to a sensor or detector for analysis. The analysis is accomplished by a sophisticated computer system that deconvolves the spectral components of the reflected light and/or any changes in intensity resulting from an index of refraction modulation. These effects can often happen simultaneously making difficult to detect and/or measure the desired effects.

SUMMARY

[0005] Embodiments of the present disclosure provide systems, devices, and methods for photodetection. For example, briefly described, in one embodiment among others, a sensor comprises an array of photodetectors, wherein the reflectance of each of the photodetectors is a function of the number of photons incident on the respective photodetector; and an electrical insulator positioned between one of the photodetectors and another one of the photodetectors to reduce diffusion of electrons therebetween.

[0006] The present disclosure can also be viewed as providing methods for sensing photons. In this regard, one embodiment of such a method, among others, can be broadly summarized by the following steps: reflecting a portion of a laser beam using a photodetector, and absorbing a plurality of photons incident upon the photodetector, thereby increasing a carrier concentration of the photodetector. The method fur-

ther comprises the step of reflecting a greater portion of the laser beam using the photodetector responsive to the absorption of the photons.

[0007] The present disclosure can also be viewed as providing embodiments of a laser resonator. In this regard, one embodiment of such a laser resonator, among others, can be broadly summarized as comprising a reflective mirror and a photodetector positioned opposite the reflective mirror. The laser resonator further comprises a lasing medium positioned between the reflective mirror and the photodetector. The reflectance of the photodetector is a function of the number of photons absorbed by the photodetector, and an intensity of a laser beam emitted by the laser resonator is a function of the reflectance of the photodetector.

[0008] The present disclosure can also be viewed as providing methods for laser doping an intrinsic semiconducting material. In this regard, one embodiment of such a method, among others, can be broadly summarized by the following steps: providing a semiconducting material having a lattice, and transmitting a laser beam to the semiconducting material in the presence of a dopant carrying gas carrying a dopant. The laser beam driving the dopant into the lattice of the semiconducting material.

[0009] The present disclosure can also be viewed as providing methods for fabricating a vertical cavity surface emitting laser (VCSEL). In this regard, one embodiment of such a method, among others, can be broadly summarized by the following steps: providing an intrinsic semiconducting material having a top surface and a bottom surface; doping the intrinsic semiconducting material to form a photodetector; depositing at least one epilayer on the top surface of the doped intrinsic semiconducting material; depositing a quantum well layer on the at least one epilayer; depositing a buffer layer on the quantum well layer; forming a pattern layer on the bottom surface of the intrinsic semiconducting material; and wet etching the intrinsic semiconducting material according to the pattern layer. The at least one epilayer provides an etch stop for wet etching the intrinsic semiconducting material, and the wet etching forms a cavity. The method further comprises depositing a distributed Bragg reflector layer in the cavity, and depositing an optically-transparent conductive film on the distributed Bragg reflector layer to form a p-side contact.

[0010] Other systems, methods, features, and advantages of the present invention will be or become apparent to one with skill in the art upon examination of the following drawings and detailed description. It is intended that all such additional systems, methods, features, and advantages be included within this description, be within the scope of the present invention, and be protected by the accompanying claims.

BRIEF DESCRIPTION OF THE DRAWINGS

[0011] Many aspects of the disclosure can be better understood with reference to the following drawings. The components in the drawings are not necessarily to scale, emphasis instead being placed upon clearly illustrating the principles of the present disclosure. Moreover, in the drawings, like reference numerals designate corresponding parts throughout the several views.

[0012] FIG. 1 is a block diagram that illustrates an embodiment of a sensor.

[0013] FIG. 2 is a block diagram that illustrates an embodiment of a system for measuring the reflectivity of a sensor.

[0014] FIG. 3 is a flowchart showing an example of a method of measuring the reflectivity of a sensor using the embodiment of the system illustrated in FIG. 2.

[0015] FIG. 4 includes four diagrams (A, B, C, and D) of semiconductor lattices that illustrate various differences between doped silicon carbide (SiC) and doped gallium nitride (GaN).

[0016] FIGS. 5A-5D, 6A-6C are block diagrams illustrating the system of FIG. 2 measuring the reflectivity of various embodiments of a sensor.

[0017] FIG. 7 is a block diagram illustrating another embodiment of a system for measuring the reflectivity of a sensor.

[0018] FIG. 8 is a graph illustrating an example of the power of a laser beam reflected by an embodiment of the sensor versus time.

[0019] FIGS. 9-11, 13-14, and 15A-15B are perspective views of various other embodiments of a sensor.

[0020] FIG. 16 is a cross-sectional view of an example of a photodiode including a capacitor.

[0021] FIG. 17 is a perspective view of an embodiment of a sensor including a plurality of vertical-cavity surface-emitting lasers (VCSELs).

[0022] FIG. 18A is a cross-sectional view of an embodiment of one of the VCSELs illustrated in FIG. 17.

[0023] FIG. 18B is a perspective view of another embodiment of one of the VCSELs illustrated in FIG. 17.

[0024] FIG. 19 is a block diagram illustrating an embodiment of a system for optically reading an embodiment of a sensor.

[0025] FIG. 20 is a block diagram illustrating an embodiment of a laser doping system.

[0026] FIG. 21 is a flowchart showing an example of a method of laser doping an intrinsic semiconducting material using the laser doping system of FIG. 20.

DETAILED DESCRIPTION

[0027] The present disclosure generally relates to systems, devices, and methods for signal amplification. Various embodiments describe photodetectors that are wireless optical photodetectors (i.e., optical signal-based photodetectors) as opposed to conventional photodetectors that are electrical signal-based photodetectors (i.e., an electrical photodetector). For example, in some embodiments, a photodetector detects incident photons by absorbing the photons, which modulates the index of refraction and reflectivity of the photodetector. The change in the index of refraction and the reflectivity of the photodetector can be monitored externally without any other active elements on the photodetector. Examples of structure, materials, and configurations of various embodiments of the sensor will be discussed below followed by a description of the fabrication and operation of the same.

[0028] FIG. 1 is a block diagram illustrating one embodiment, among others, of a sensor 100, denoted herein as 100a. The sensor 100a, includes a photodetector 104, which includes a doped region of an intrinsic semiconductor material 102. The doped region may be p-doped or n-doped. In other embodiments, which will be discussed in further detail below, the sensor 100 may include an array of photodetectors 104. A photodetector 104 absorbs at least some of the photons 110 incident upon the photodetector 104, which alters the carrier concentration of the photodetector 104. The change in the carrier concentration results in a change in the index of

refraction and the reflectivity of the photodetector 104. The level of doping affects the absorption level of the photodetector 104 as well as the amount of change in reflectivity. Various other embodiments of sensors 100 including at least one photodetector 104 which will be discussed in further detail below.

[0029] FIG. 2 is a block diagram illustrating one embodiment, among others, of a system 200 for measuring the reflectivity of a sensor 100. Specifically, the system 200, denoted herein as 200a, is for measuring the reflectivity of the photodetector 104 included within a sensor 100 and, thus, photons 110 incident upon the photodetector 104. In the embodiment illustrated in FIG. 2, the sensor 100 measured is the sensor 100a illustrated in FIG. 1. A laser beam 204, such as a helium-neon (He—Ne) laser beam, passes through a beam splitter 206 and is incident upon the photodetector 104. The laser beam 204 is reflected by the photodetector 104 back up to the beam splitter 206, which reflects and redirects the laser beam 204 to a power meter 212, denoted herein as reflected laser beam 210.

[0030] FIG. 3 is a flowchart showing an example of a method 300 of measuring the reflectivity of a sensor 100 using the embodiment of the system 200a illustrated in FIG. 2. In box 302, a laser beam 204 is transmitted to a photodetector 104. In some embodiments, such as the one illustrated in FIG. 2, the laser beam 204 is transmitted through a beam splitter 206. In box 304, a portion of the laser beam 204 is reflected by the photodetector 104. The reflected portion of the laser beam 204 is shown as reflected laser beam 210 in the example illustrated in FIG. 2. In box 306, the reflected laser beam 210 is redirected to a power meter 212 by the beam splitter 206.

[0031] In box 308, the power meter 212 senses a power associated with the reflected laser beam 210. In box 310, a plurality of photons 110 that are incident upon the photodetector 104 are absorbed by the photodetector 104. Not all photons 110 that are incident on the photodetector 104 are absorbed. Only the photons 110 having a wavelength (or frequency) that corresponds to bandgap of the photodetector 104 are absorbed, which will be discussed in further detail below. The absorption of photons 110 by the photodetector 104 increases the carrier concentration of the photodetector 104.

[0032] In box 312, a greater portion of the laser beam 204 is reflected by the photodetector 104 responsive to the absorption of the photons 110. In box 314, an increase in the power associated with the reflected laser beam 210 is sensed by the power meter 212. Accordingly, subtle changes in reflectivity due to a small number of photons 110 incident upon the photodetector 104 can be detected. In some embodiments, the system 200a may be configured to measure the reflectivity of each photodetector 104 in an array of photodetectors 104.

[0033] Having generally described the structure and measurement of the reflectivity of an embodiment of a sensor 100, examples of materials of various embodiments of a sensor 100 will now be discussed. Referring to FIG. 1, the intrinsic semiconducting material 102 may be silicon carbide (SiC), gallium nitride (GaN), silicon (Si), gallium arsenide (GaAs), and/or another intrinsic semiconductor material. Further, the intrinsic semiconducting material 102 may be doped with gallium (Ga), boron (B), aluminum (Al), indium (In), thallium (Tl), and/or another p-type dopant. Doping provides a specific wavelength sensitivity based on the dopant selected, and doping also creates a region of high electron mobility in

the photodetector **104** relative to the intrinsic semiconducting material **102**. In some embodiments, the intrinsic semiconducting material **102** may be doped with multiple p-type dopants.

[0034] In some embodiments, SiC may be preferable to GaN as the intrinsic semiconducting material **102** for several reasons, which will be discussed in the following paragraphs. For example, SiC may be preferable as the intrinsic semiconducting material **102** because SiC forms covalent bonds with the dopants instead of polar bonds. FIG. 4 includes four diagrams (A, B, C, and D) of semiconductor lattices that illustrate the differences between doped SiC and doped GaN. Beginning with FIG. 4(A), shown is a diagram of an example of a SiC lattice doped with nitrogen (N). N creates n-type doping in both silicon (Si) and carbon (C) lattice sites. Next, in FIG. 4(B), shown is a diagram of an example of a SiC lattice doped with gallium (Ga). Ga creates p-type doping in both Si and C lattice sites. Since SiC forms covalent bonds, SiC allows n-type or p-type doping regardless of whether the dopant atoms occupy the Si or C sites in the SiC lattice.

[0035] In contrast, for example, GaN is a less ideal intrinsic semiconducting material **102** than SiC for creating a sensor **100** because the polar bonds in GaN cause ambiguous n-type or p-type doping depending on whether the dopant atoms occupy the Ga or N sites in the GaN lattice. For example, in FIG. 4(C), shown is a diagram of a GaN lattice doped with Si. As can be seen in FIG. 4(C), the Si atom in a Ga site in the GaN lattice contributes an electron and provides n-type doping whereas the Si in the N site in the GaN lattice contributes a hole and, thus, provides p-type doping. Accordingly, doping a GaN lattice with Si results in ambiguous doping since the Si may contribute either a hole or an electron. Similarly, in FIG. 4(D), shown is a diagram of an example of a GaN lattice doped with magnesium (Mg). As can be seen in FIG. 4(D), the Mg atom in a Ga site in the GaN lattice contributes a hole and provides p-type doping, but the Mg atom in a nitrogen (N) site in the GaN lattice contributes three holes per dopant atom. The Mg atom in the N site can act as a trap or a nonradiative recombination center.

[0036] Another reason that SiC may be preferable as the intrinsic semiconducting material **102** for the photodetector **104** over GaN is because of the low ionization of acceptors in GaN. Specifically, when GaN is doped with Mg, less than 10% of the Mg atoms are expected to ionize in GaN. So, for GaN, the concentration of Mg would have to be about two orders of magnitude larger than a desired hole concentration.

[0037] As still another reason that SiC may be preferable as the intrinsic semiconducting material **102** over GaN is because manufacturing SiC is easier. For example, single crystal SiC wafers are available in large diameters (e.g., 3"-4"). Additionally, focal plane arrays and other devices can also be built on a single SiC chip. Moreover, although GaN is available in polycrystalline thin films, thin GaN films often contain numerous defects that can act as thermal absorbers in the infrared (IR) and mid-wave infrared (MWIR) ranges. Also, although SiC crystals tend to have micropipe and dislocation defects, the number of these defects per unit area has been reduced significantly by improvements in crystal growth processes.

[0038] Additionally, for embodiments of the sensor **100** including an array of photodetectors **104**, SiC may be preferable as the intrinsic semiconducting material **102** because electrons and holes have lower mobility and diffusion coefficients in SiC than other intrinsic semiconductor materials

102. Consequently, the loss of signal due to diffusion of electrons to neighboring photodetectors **104** in an array is lower when the lattice material is SiC instead of GaN, Si, and/or gallium arsenide (GaAs). Such loss of signal may reduce the contrast of an image. The level of doping affects the absorption level of the frequency of light from a radiation source and the subsequent amplitude of free carriers and the amount of change in reflectivity.

[0039] Having generally described the structure and materials of an embodiment of a sensor **100**, the mechanism within the photodetector **104** resulting in photodetection will be discussed in connection with FIGS. 5A-5D, 6A-6C. FIG. 5A is a block diagram illustrating an example of the system **200a** for measuring the reflectivity of a photodetector **104** included within a sensor **100**, similar to the system illustrated in FIG. 2. As in FIG. 2, the example of a sensor **100**, denoted as **100a**, is illustrated as being measured by the system **200a**. Also, similar to the system **200a** of FIG. 2, the system **200a** illustrated in FIG. 5A reflects and redirects the incident laser beam **204** as shown by the reflected laser beam **210**.

[0040] However, in the embodiment illustrated in FIG. 5A, the sensor **100a** includes an example of an energy band diagram corresponding to an example of a photodetector **104**, denoted herein as **104a**. The energy band diagram of the photodetector **104a** includes a valence band (E_v), a conduction band (E_c), and an acceptor band (E_a), which is an energy band associated with an acceptor (i.e., p-type) dopant. The energy gap (E_g) is determined by E_a and E_v , and hence the selection of the acceptor dopant for the intrinsic semiconducting material **102**. As discussed above, in some embodiments, the sensor **100** is a Ga-doped SiC, and in those embodiments, the energy band level is determined by Ga.

[0041] FIG. 5B is another block diagram illustrating the example of the system **200a** shown in FIG. 5A including photons **110** incident upon the sensor **100a**. Since the wavelengths associated with the photons **110** do not correspond to the energy gap E_g , the photons **110** are not absorbed by the photodetector **104a** and, thus, not detected. Further, the reflectivity of the photodetector **104a** remains unchanged, and the intensity of the reflected laser beam **210** remains unchanged as well.

[0042] FIG. 5C is yet another block diagram illustrating the example of the system **200a** shown in FIG. 5A including a photon **110** incident upon the sensor **100a**. However, in FIG. 5C, the incident photon **110** has a wavelength λ_g that corresponds to the energy gap E_g , and the photodetector **104a** absorbs the photon **110**, causing an electron to be promoted from the valence band E_v to the acceptor band E_a . The promotion provides an increase in holes, which alters the carrier concentration of the photodetector **104a**. The change in carrier concentration, in this example, increases the reflectivity of the photodetector **104a**, causing the intensity of the reflected laser beam **210** to increase. This increase is then detectable by the power meter **212**. Accordingly, a photodetector **104a** may be tuned to detect photons **110** having a particular frequency, which is a function of the wavelength and the speed of light, based at least in part on the dopant.

[0043] FIG. 5D is still another block diagram illustrating the example of the system **200a** shown in FIG. 5A including photons **110** having wavelength λ_g incident upon the sensor **100a**. Since more photons **110** are absorbed than illustrated in FIG. 5C, the intensity of the reflected laser beam **210** is further increased. Accordingly, since the intensity of the reflected laser beam **210** is directly correlated with the num-

ber of incident photons **110**, the system **200a** is sensitive to how many photons **110** are incident upon the photodetector **104a**.

[0044] Turning now to FIG. 6A, shown is a block diagram illustrating an example of the system **200a** for measuring the reflectivity of a photodetector **104** included within a sensor **100**, similar to the system illustrated in FIG. 2. Similar to FIG. 2, the example of a sensor **100**, denoted as **100a**, is illustrated as being measured by the system **200a**. Also, similar to the system **200a** of FIG. 2, the system **200a** illustrated in FIG. 5A reflects and redirects the incident laser beam **204** as shown by the reflected laser beam **210**.

[0045] However, in the embodiment illustrated in FIG. 6A, the sensor **100a** includes an example of an energy band diagram corresponding to an example of a photodetector **104**, denoted herein as **104b**. Similar to the energy band diagram of the photodetector **104a** illustrated in FIGS. 5A-5D, the energy band diagram of the photodetector **104b** includes a valence band (E_V) and a conduction band (E_C). However, the energy band diagram of photodetector **104b** also includes multiple energy bands E_1, E_2 associated with various dopants. Additionally, an energy difference ΔE is defined by the energy bands E_1, E_2 .

[0046] As an example, in some embodiments, the sensor **100** includes SiC as the intrinsic semiconducting material **102**, which is doped with aluminum (Al) and Ga. The Al dopant defines the energy band E_1 (about 0.27 eV from the valence band E_V), and the Ga dopant defines the energy band E_2 (about 0.29 eV from the valence band E_V). This means that ΔE is about 20 meV, which corresponds to a frequency of about 5 THz. In other embodiments, the SiC is doped with boron (B) and Ga. In those embodiments, the B dopant defines the energy band E_1 (about 0.29 eV from the valence band E_V), and the Ga dopant defines the energy band E_2 (about 0.30 eV from the valence band E_V). Accordingly, in embodiments where the sensor **100** includes SiC doped with B and Ga, the ΔE is about 10 meV, which corresponds to a frequency of about 2.5 THz.

[0047] Moving now to FIG. 6B, shown is another block diagram illustrating the example of the system **200a** shown in FIG. 6A including the sensor **100a**. In FIG. 6B, the photodetector **104b** in the sensor **100a** is biased such that at least some of the electrons are promoted from the valence band E_V to the energy band E_1 . The biasing increases the reflectivity of the photodetector **104b**, causing the intensity of the reflected laser beam **210** to increase.

[0048] FIG. 6C is still another block diagram illustrating the example of the system **200a** shown in FIG. 6A including the sensor **100a**. In FIG. 6C, the photodetector **104b** in the sensor **100a** is biased as shown in FIG. 6B, and photons **110** having a wavelength λ_A that corresponds to the energy difference ΔE are incident upon the photodetector **104b**. The photodetector **104b** absorbs the photons **110**, which causes electrons to be promoted from energy band E_1 to energy band E_2 . This promotion causes the reflectivity of the photodetector **104b** to increase further and, thus, increase the intensity of the reflected laser beam **210** further. Accordingly, the sensors **100a** described in FIGS. 6A-6C are capable of detecting photons **110** having frequencies of about 2.5 or 5 THz, depending on the selection of dopants.

[0049] FIG. 7 is a block diagram illustrating another embodiment, among others, of a system **200** for measuring the reflectivity of a sensor **100**. Specifically, the system **200**, denoted herein as **200b**, is for measuring the reflectivity of the

photodetector **104** included within a sensor **100**, denoted herein as **100b**. The sensor **100b** is sensitive to incident particles or radiation from a nuclear source, and the reflectivity of the photodetector **104** included within the sensor **100b** changes responsive to the incident particles or radiation.

[0050] The sensor **100b** includes a photodetector **104**, an attenuator layer **706**, and a converter layer **703** therebetween. The photodetector **104** includes a layer of p-type SiC, and the converter layer **703** includes an n-type wide bandgap material having a high capture cross section for nuclear particles or radiation. The attenuator layer **706** slows down the incident particles or radiation.

[0051] The converter layer **703** is so chosen that its capture cross section is very high for the particles and/or radiation to be detected. Since the capture cross section is generally very high for thermal neutrons or low energy γ rays, the attenuator layer **706** would be unnecessary for detecting such low energy particles or radiations. To achieve high sensitivity of the detector for detecting fast neutrons or high energy γ rays, the attenuator layer **706** would be necessary to slow down the incident particles and/or radiations so that they can be absorbed by the converter layer **703** with high capture cross section.

[0052] To detect neutrons or γ rays selectively, an absorber layer can be deposited on the attenuator layer **706**. This selectivity can be achieved by considering an absorber layer, which preferentially captures or attenuates neutrons or γ rays, and by designing the thickness of the absorber layer appropriately. The absorber layer will act as a nuclear filter. For example, an absorber layer of zirconium dioxide (ZrO_2) or tungsten oxide (W_2O_3) will filter out the γ rays, while passing the neutrons to the attenuator layer **706**. Similarly, an absorber layer of boron carbide (BC), boron nitride (BN) or gadolinium carbide (GdC) will filter out neutrons, while passing the γ rays to the attenuator layer **706**. In contrast to this selective detection approach, two lasers of different wavelengths can be used to measure the reflectivity of the photodetector **104** at these two wavelengths and then decouple the signals to detect neutrons and γ rays simultaneously.

[0053] The photodetector **104** (e.g., p-type SiC) and converter layer **703** (e.g., n-type region) produce a p-n junction diode with a built-in electric field and distributions of electrons and holes in the depletion layer as shown in FIG. 7, for example. This p-n junction interface provides a controlled location where the charged particles produced by neutrons and γ rays will interact with the electrons and holes and, consequently, modify the densities of the electrons and holes in various energy levels. The optical property, particularly the reflectivity of the interface, can be related to the number density of charged particles at the interface, which in turn can be related to the neutron flux or the intensity of the γ rays incident on the converter layer **703** or the attenuator layer **706** or the absorber layer. Thus, a change in the interfacial reflectivity provides an optical detection mechanism.

[0054] Brand et al. investigated Gd-rich oxide/Si heterojunction diodes to detect neutrons by considering the fact that the charged particles produced by neutrons generate electrical signals in the diode. (See J. Brand, M. Natta, P. Jeppson, S. Balkir, N. Schemm, K. Osberg, D. Schultz, J. C. Petrosky, J. W. McClory, J. Tang, W. Wang and P. A. Dowben, Gadolinium rich oxide/silicon heterojunction diodes for solid state neutron detection, World Journal of Engineering, 2009, Vol. 6 (Supplement), pp. 91-92.) The sensor **100b** described herein uses silicon carbide instead of Si because SiC is highly resis-

tant (rad hard) to radiation damage. Also, the optical detection mechanism of sensor **100b** provides a wireless, remote sensing capability. Additionally the converter layer **703**, attenuator layer **706**, and absorber layers may each include ceramics, such as oxides, carbides and nitrides, which are high temperature materials. SiC is a wide bandgap semiconductor with bandgap energy (3.26 eV for 4H—SiC) much higher than those of the conventional Si (1.12 eV) and Ge (0.67 eV) semiconductors. Therefore the sensor **100b** described herein is suitable for high temperature applications compared to conventional semiconductor-based detectors.

[0055] The choice of materials for fabricating a sensor **100b** depends on the energy of the nuclear particles or radiations to be detected and how the nuclear particles or radiations interact with the material to form charged particles. P-type SiC substrates can be fabricated by doping SiC with aluminum, while Gd₂O₃ intrinsically exhibits n-type characteristics due to oxygen vacancies.

[0056] In some embodiments, the sensor **100b** is designed to detect neutrons. A material of high neutron capture cross section is included in the sensor **100b** for detecting both slow and fast neutrons. The mechanism involves both the scattering and ionizing effects of neutrons in the case of detecting fast neutrons. Gadolinium has an isotope ¹⁵⁷Gd with thermal neutron capture cross section 255000 barns, which is much higher than the cross sections of 3840 barns for ¹⁰B and 940 barns for ⁶Li. The natural abundances of ¹⁵⁷Gd, ¹⁰B and ⁶Li are 15.7, 19.8 and 7.4 at. % respectively. The thermal neutron capture cross section of natural Gd is 46000 barns, which is also significantly high. It should be noted that the neutron capture cross sections of these isotopes decrease to very low values when the neutron energy increases. The neutron capture cross section of Gd is, however, known to be significant up to about 200 MeV.

[0057] For detecting fast neutrons, the attenuator layer **706** can be a graded structure or a multilayered heterogeneous structure consisting of Gd₂O_{3(1-x)}C_{2x} with x increasing from about 0 at the p-n junction interface to about 1 at the free surface of the attenuator layer **706**. When a flux of fast neutrons is incident on the free surface of the attenuator layer **706**, the carbon atoms will reduce the energy of neutrons through elastic and inelastic scattering, resulting in the arrival of slow neutrons at the converter layer **703**. Therefore the high cross section of Gd will be utilized to capture these slow neutrons, resulting in high sensitivity of the sensor **100b**.

[0058] In some embodiments, the sensor **100b** is designed to detect γ rays. γ rays interact with materials through three mechanisms: photoelectric effect, Compton scattering, and pair production. In the photoelectric effect, which occurs for the γ ray energies up to about 200 keV, the γ photon transfers all of its energy to an atomic electron with interaction cross section proportional to NZ^5 , where N and Z are the number of atoms per unit volume and the effective atomic number of the material respectively. In the Compton effect, which occurs for the γ ray energies up to a few MeV, the γ photon transfers a fraction of its energy to an outer electron with interaction cross section proportional to NZ , resulting in a hot (high energy) electron and a photon of energy lower than that of the incident γ photon. The pair production, which occurs for γ ray energies above 1.02 MeV, involves interactions between the γ photon and the Coulomb field of the nucleus with interaction cross section proportional to NZ^2 , resulting in the production of an electron and a positron.

[0059] Due to the large influence of atomic number on the interaction cross section, the converter layer **703** can be constructed using a rad hard material of high atomic number, such as ZrO₂, for γ ray detection. Since the neutron capture cross section of Zr is very low, the ZrO₂ converter layer is not expected to produce significant signals for neutrons, instead it will yield signals for γ rays.

[0060] Possible applications of the sensor **100b** and/or the system **200b** include the control and monitoring of nuclear reactors and fuel processing, characterization of nuclear fuel rods and detection of concealed fissile and radioactive materials.

[0061] Having generally described the structure, materials, and mechanisms of various embodiments of a sensor **100**, various figures of merit gathered from experimental results will be discussed in the following paragraphs. Specifically, experimental results have been collected for a sensor **100** including an intrinsic semiconducting material **102** of SiC having a region doped with Ga to form a photodetector **104**. Among the various figures of merit are detectivity (D*) and noise equivalent temperature difference (NETD), which can be calculated based at least in part on the power of the reflected laser beam **210**. D* is a measurement of the sensitivity (S) of an active area of 1 cm² of the photodetector at a 1 Hz noise-equivalent bandwidth. For conventional electrical photodetectors, the S is a voltage (or current) produced by the electrical photodetector per watt of incident energy [V/W]. For a wireless optical photodetector, such as the photodetector **104**, the S is a change in reflectance of the wireless optical photodetector per watt of incident energy [W⁻¹].

[0062] FIG. 8 is a graph illustrating an example of the power of the reflected laser beam **210** (e.g., a He—Ne laser beam) reflected by an embodiment of the photodetector **104** versus time. The power of reflected laser beam **210** is measured by the power meter **212** in the system **200a** illustrated in FIG. 2. As discussed above, the power of the reflected laser beam **210** is a function of the modulation of the index of refraction of the photodetector **104** caused by absorbed photons **110**. The graph also illustrates the reflected power various temperatures of the source, and the temperatures are useful in determining NETD. T_{BG} is the background temperature of other materials surrounding the source, and in this study, T_{BG} is 25° C., and the reflected power is lower than that of the source due to the difference in emissivity. NETD can be determined from the experimental data of statistical consideration using as shown in Equation (1):

$$NETD = \frac{\sigma_n}{SITF} \quad (1)$$

where σ_n is the standard deviation of the detector signal and SITF is the system intensity transfer function. SITF is calculated as shown in Equation (2):

$$SITF = \frac{\bar{P}_2 - \bar{P}_1}{T_2 - T_1} \quad (2)$$

where P₁ and P₂ are the powers of the reflected laser beam **210** (i.e., the reflected power of He—Ne beam) measured at dif-

ferent times for the source temperatures of T_1 and T_2 , respectively. Further, the detectivity of the sensor **100** can be calculated by the equation bellow.

$$D^* = \frac{(S/N)}{\rho_{d,l}^* I_{i,l}^*} \sqrt{\frac{\Delta f}{A_{Si}}} \quad (3)$$

[0063] where S/N is the signal-to-noise ratio of the photodetector **104**; Δf is the bandwidth of the output circuit [Hz]; $I_{i,l}^*$ is the irradiance of the reflected laser beam **210** incident on the photodetector **104** in the presence of MWIR source [W/cm^2]; and A_{Si} is the effective area of the photodetector **104** [cm^2]. For the photodetector **104**, $I_{i,l}^*$ is calculated to be 26.786 nW/mm^2 and A_{Si} is calculated to be 1.131 mm^2 .

[0064] Based on the measurements taken at T_{BG} equal to 25° C. , the noise (N) of the signal, which is the standard deviation of the fluctuations in electrical output of the He—Ne beam detector, the signal-to-noise ratio (S/N) is calculated based on $N=1.778 \times 10^{-9}$. $S/N=P_{\text{signal}}/P_{\text{noise}}=423.51$ and $\Delta f=2.5 \times 10^5 \text{ Hz}$ for a photodetector (He—Ne beam detector) and power meter system (e.g., Newport photodetector of model No. 818-SL equipped with 842-PE power meter).

[0065] For calculating detectivity of photons **110** in the MWIR range, the parameter, $\rho_{d,l}^*$, which is the reflectance of the photodetector **104** for the He—Ne laser wavelength in the presence of MWIR irradiance, is 0.28. This produces a theoretical result of detectivity for the photodetector system consisting of photodetector **104** made of Ga-doped SiC and the He—Ne beam detector and power meter system of $\Delta f=2.5 \times 10^5 \text{ Hz}$.

$$D^* = \frac{(423.51)\sqrt{2.5 \times 10^5 \text{ Hz}}}{(0.28)(2.679 \times 10^{-6} \text{ W/cm}^2)\sqrt{(1.131 \times 10^{-2} \text{ cm}^2)}} \quad (4)$$

$$= 2.7 \times 10^{12} \text{ cm}\sqrt{\text{Hz}}/\text{W}$$

[0066] Accordingly, the photodetector **104** including Ga doped SiC has a theoretical detectivity of $D^*=2.857 \times 10^{12} \text{ cm}\sqrt{\text{Hz}}/\text{W}$ and NETD of 39 mK. However, the experimental NETD is 396 mK for certain embodiments of the photodetector **104**, specifically, for the photodetector system consisting of photodetector **104** made of Ga-doped SiC, and the He—Ne beam detector and power meter system of $\Delta f=50 \text{ Hz}$, and a lens system that collects more MWIR photons from the field of view and then focuses the collected photons onto the photodetector **104** with increased intensity. Additional sensitivity can be obtained by growing nanostructures on the photodetector **104**. Nanostructures have been shown to increase the surface area of materials enhancing the interaction with light. Note in a sensor **100** having an array of photodetectors **104**, the absolute surface area will vary from photodetector **104** to photodetector **104**, if nanostructures are included. This means that the absolute sensitivity and signal will vary from photodetector **104** to photodetector **104**. This variation may be addressed by a process that is standard within the infra red imaging and detection technology of normalization. Normalization of an array of a photodetectors **104** is accomplished by uniformly illuminating the array measuring the response of each photodetectors **104**. The lowest performing photodetectors **104** becomes the standard by which the other photode-

tectors **104** in the array are referenced. The brighter or more sensitive photodetectors **104** have their signal subtracted via a microprocess controlled algorithm. This diminishes the overall array sensitivity but enables a uniform response for the output array for detection and quantitative analysis. Different dopants enable the photodetectors **104** to sense different frequencies of light.

[0067] The experimental results indicate that, in some embodiments, the photodetector **104a** has an NETD of 339 mK. Traditional infrared detectors reach NETD of about 10 mK, but traditional infrared detectors also typically have integrated circuit amplifiers or gain elements on the same microchip as the detector to provide several orders of magnitude of amplification of the signal before being transmitted. In contrast, various embodiments of the sensor **100** described in the present application do not require active elements. Hence, the sensor **100** in those embodiments does not suffer from problems such as thermal run away, which can cause a detector to be inoperative in harsh environments. Moreover, in embodiments where batteries are not necessary, the sensor **100** can operate for an indefinite period of time.

[0068] FIG. 9 is a block diagram illustrating another embodiment, among others, of a sensor **100**, denoted herein as **100b**. In this embodiment, the sensor **100b** includes an array of photodetectors **104** (e.g., pixels). The array configuration enables the sensor **100b** to detect photons **110** in various positions across the sensor **100b**, and an image associated with the detected photons **110** in the various positions may be formed. As briefly mentioned above, the array of photodetectors **104** are formed by doping a wafer of an intrinsic semiconducting material **102** according to pattern defined by a mask to form an array of photodetectors **104**. In the embodiment illustrated, the photodetectors **104** are spaced such that the intrinsic semiconducting material **102** borders each photodetector **104**, which reduces the diffusion of electrons between neighboring photodetectors **104**. Diffusion of electrons between photodetectors **104** can degrade the integrity of the signals provided by the photodetectors **104**.

[0069] Other structural features may be incorporated into a sensor **100** to reduce diffusion of electrons between neighboring photodetectors **104**. For example, in some embodiments, an electrically insulating material such as silicon dioxide may be positioned between a photodetector **104** and a neighboring photodetector **104** to reduce diffusion therebetween. As another example, a via trench may be etched between at least one of the photodetectors **104** and a neighboring photodetector **104** to provide air as the insulator. In some embodiments, the electrically insulating material, metal, or via trenches may surround the perimeter of a photodetector **104** to prevent diffusion of electrons between photodetectors **104**. In some embodiments, the intrinsic semiconducting material **102** between neighboring photodetectors **104** may be processed with a chemical that reduces the diffusion of electrons between photodetectors **104**.

[0070] FIG. 10 illustrates another embodiment of a sensor **100**, denoted herein as **100c**. The sensor **100c** includes an array of photodetectors **104** and a metal grid **1002** positioned between the photodetectors **104** that is connected to ground **1004** to route electrons that diffuse between the photodetectors **104** to ground **1004**. In other embodiments, a metal barrier connected to ground **1004** may be positioned between at least some of the photodetectors **104** in another configuration.

[0071] FIG. 11 illustrates still another embodiment of a sensor 100, denoted herein as 100d. In FIG. 11, the sensor 100d includes an array of various examples of photodetectors 104, denoted herein as 104c, 104d, 104e, and 104f. Each of the photodetectors 104c, 104d, 104e, and 104f may be doped such that the photodetectors 104c, 104d, 104e, and 104f are responsive to photons 110 having different wavelengths. In this example, the various photodetectors 104 are grouped in groups 1102 of four photodetectors 104, which forms an array of groups 1102 of photodetectors 104. In other embodiments, the various photodetectors 104 may be grouped in a different manner, and each group 1102 may include more or less than four different photodetectors 104.

[0072] FIG. 12 is a cross-sectional view of a further embodiment of a sensor 100, denoted herein as 100e. The sensor 100e is similar to the sensor 100b illustrated in FIG. 9 in that the sensor 100e includes an array of photodetectors 104. The sensor 100e further includes an optically-transparent conductive film 1202 that covers the top of each photodetector 104. A direct current (DC) voltage may be applied to the optically-transparent conductive film 1202 to sweep away the free photogenerated carriers, which enhances the lifetime of the photogenerated carriers, and hence the reflectivity of the modulated signal.

[0073] In some embodiments, less than the entire top surface of each photodetector 104 may be covered by the optically-transparent conductive film 1202. Also, in some embodiments, at least a portion of the intrinsic semiconducting material 102 may be covered by the optically-transparent conductive film 1202 as well. The optically-transparent conductive film 1202 may include a material that is transparent in the mid infrared range, such as Indium Tin Oxide (ITO), and the optically-transparent conductive film 1202 may be deposited by a DC or RF sputtering system at pressures on the order of μTorr at a deposition rate of 10 $\text{\AA}/\text{minute}$. An additional thermal treatment in air may also be applied to enhance the conductivity and transparency of the optically-transparent conductive film 1202. For ITO, a typical thermal anneal is 400° C. for about 30 minutes.

[0074] FIG. 13 is a block diagram illustrating another embodiment of a sensor 100, denoted herein as 100f. The sensor 100f includes an avalanche photodiode 1302 that includes an n-type region 1304 and a p-type region 1303 forms photodetector 104. In other embodiments, avalanche photodiode 1302 may include a p-type region 1303, and the n-type region 1304 may form the photodetector 104. An external electric field is applied across the avalanche photodiode 1302. In some embodiments, a sensor 100 may include an array of avalanche photodiodes 1302, each including a photodetector 104 and being biased by an external electric field.

[0075] The external electric field removes photoexcited electrons from the acceptor band E_a (dopant energy level) in the photodetector 104 and accelerates the photoexcited electrons toward the cathode 1306. This causes some of the photogenerated electrons to jump back to the valence band E_v and recombine with holes. This generation-recombination process establishes an equilibrium electron population density in the acceptor band E_a . Removal of electrons from the acceptor band E_a by the external electric field creates a nonequilibrium mechanism to produce vacant sites for electrons in the acceptor band E_a in the photodetector 104, enabling the incident

photons 110 to generate more photoexcited electrons. This nonequilibrium mechanism can increase the quantum efficiency of the sensor 100f.

[0076] Also, the external electric field causes the accelerated electrons to collide with other electrons to produce hot electrons (i.e., highly energetic free electrons). These hot electrons also collide with other electrons and produce more hot electrons, leading to an avalanche of electrons. Therefore, the free electron density will increase in the photodetector 104, causing a large change in the reflectivity of the sensor 100f. This large change in reflectivity enables the photodetector 104 to detect of a weak signal (very few photons) from a target. In some embodiments, the sensor 103 may be included in another electronic device, such as a transistor.

[0077] FIG. 14 is a block diagram illustrating an example of a sensor 100g that includes a laser resonator 1401. The laser resonator 1401 includes a fully reflective mirror 1404, a lasing medium 1406, and a photodetector 104 that functions as a mirror having a variable reflectivity. The dichroic mirror 1402 is positioned in front of the photodetector 104, and the dichroic mirror 1402 allows photons 110 to pass through the dichroic mirror 1402 to the photodetector 104. However, the dichroic mirror 1402 fully reflects the laser beam coming out of the laser resonator 1401. The photoexcited electrons modify the electron density in the photodetector 104, which changes the refractive index and, consequently, the reflectivity of the photodetector 104. This change in reflectivity modifies the intensity of the laser beam 1410 leaving the laser resonator 1401. By this mechanism, the sensor 100g can detect a very weak signal (e.g., very few photons 110) and obtain a strong optical (e.g., laser) signal based on the photodetector 104 response. The optical signal can be used to produce images in flat panel displays or on another screen.

[0078] In some embodiments, the photodetector 104 of the laser resonator 1401 may be included within an avalanche photodiode 1302, such as the avalanche photodiode 1302 illustrated in FIG. 13, and/or another electronic device to enhance the production of electrons in different energy levels in order to cause a large change in reflectivity of the photodetector 104. In those embodiments, the avalanche photodiode 1302 is biased as illustrated in FIG. 13. A large change in the reflectivity of the photodetector 104 causes a greater change in the laser power exiting the laser resonator 1401, and thus, amplifies the signal even further. In some embodiments, the sensor 100g may include an array of laser resonators 1401.

[0079] FIGS. 15A-15B are block diagrams illustrating examples of a sensor 100, denoted herein as 100h and 100i, respectively. The sensors 100h, 100i each include a circuit 1501, denoted herein as 1501h and 1501i, respectively, that couple a laser source 1504 to an example of a photodiode 1502 including a photodetector 104, denoted herein as 1502a. The photodiode 1502a may be a p-n junction diode, PIN diode, or another diode structure.

[0080] In the embodiments illustrated, the photodiode 1502a includes a p-type doped region 1509 and an n-type region 1506. In some embodiments, such as the ones illustrated in FIGS. 15A-15B, the p-type region 1509 forms the photodetector 104. In other embodiments, the n-type region 1506 forms the photodetector 104. A depletion region 1508 is formed at the junction of the p-type region 1509 and the n-type region 1506 with a built-in electric field across the depletion region 1508. The direction of this built-in electric field is from the interface between the depletion region 1508

and the n-type doped region **1506** to the interface between the depletion region **1508** and the photodetector **104**. The photodiode **1502a** is reverse-biased by a voltage source **1516**.

[0081] The photoexcited electrons are produced in the photodetector **104**, and the photoexcited electrons travel toward the n-type doped region **1506** of the photodiode **1502a** due to the built-in electric field in the depletion region **1508**. These electrons are moved through the electrical circuit **1501** by the external voltage source **1516**, establishing photocurrent in the circuit **1501**. The creation of photoexcited electrons by the photons **110** effectively reduces the resistance of the photodiode **1502a**, inducing photocurrent in the circuit **1501**. The external voltage source **1516** is also coupled to a laser source **1504** that is forward biased. This laser source **1504** is a p-n junction light-emitting device, a laser diode, a quantum well device, and/or another laser-producing device, and the laser source **1504** emits a laser beam **1511**.

[0082] In the embodiment illustrated in FIG. **15A**, the laser source **1504** is coupled in parallel with the photodetector **104** and the external voltage source **1516**. However, in the embodiment illustrated in FIG. **15B**, the photodetector **104** is connected in series with the laser source **1504** and the external voltage source **1516**. In the absence of photoexcitation due to incident photons **110**, the resistance of the photodetector **104** is high, which affects the overall resistance of the circuit **1501**. When photons **110** are incident on the photodetector **104**, the resistance of the photodetector **104** decreases, which changes the overall resistance of the circuit **1501**. Consequently, the number of electrons and holes injected into the laser source **1504** by the external voltage source **1516** changes, which modifies the output laser power (i.e., output signal). Accordingly, an optical signal can be produced based on the photodetector **104** response to the incident photons **110** (i.e., input signal), and the optical signal can be used to display images of a target that emitted the photons **110** in a flat panel display or another screen.

[0083] In some embodiments, the sensors **100h**, **100i** include an array of photodiodes **1502a** and an array of laser sources **1504**. Each photodiode **1502a** is coupled to a respective one of the laser sources **1504**. In some embodiments, the external voltage source **1516** is an AC voltage source instead of a DC voltage source. In those embodiments, the AC voltage source is used to create a pulsed photocurrent and a pulsed laser beam **1511** (i.e., a pulsed optical signal output). For a small amount of energy per pulse, the intensity of the laser beam **1511** is very high which enables amplification of weak incident signals. Resistors (e.g., R_1 , R_2), capacitors, and inductors can be used in the circuits **1501h**, **1501i** to create an oscillation frequency for absorbing more of the incident photons **110** by the photodiode **1502a**.

[0084] FIG. **16** is a cross-sectional view of another example of a photodiode **1502**, denoted herein as **1502b**, further including a capacitor **1602**. For example, in FIG. **16**, an example of a capacitor **1602**, denoted **1602a**, is formed on the photodetector **104** of the photodiode **1502**. The capacitor **1602a** includes a first metal layer **1604** and a second metal layer **1606** having an insulating layer **1608** (e.g., silicon dioxide) therebetween. The first metal layer **1604** is deposited on the photodetector **104**, and the insulating layer **1608** is deposited on the first metal layer **1604**. The insulating layer **1608** may be deposited by a plasma-enhanced chemical vapor deposition (PECVD), sputtering, or another deposition process. In some embodiments, the insulating layer **1608** is at least about 500 Å thick. The second metal layer **1606** is

deposited on the insulating layer **1608** and an additional insulating layer **1613** that abuts the photodetector **104**. The photoexcited electrons can be stored in this capacitor **1602a**. Accordingly, the electron density in selected regions of the photodiode **1502** may be modified depending on the locations of the capacitor **1602a** in the photodiode **1502**. Therefore, the refractive index of the photodetector **104** can be changed selectively based on the electron storage capability of the capacitor **1602a**, which will increase the sensitivity of the photodetector **104**. In other embodiments, a plurality of capacitors **1602** may be fabricated in the photodiode **1502**.

[0085] FIG. **17** illustrates another embodiment of a sensor **100**, denoted herein as **100j**. The sensor **100j** includes an array of vertical-cavity surface-emitting lasers (VCSELs) **1701**, and each VCSEL includes a photodetector **104**. Not only may a VCSEL **1701** increase the gain of a photodetector **104**, but the signal-to-noise ratio of the photodetector **104** may be enhanced by including the photodetector **104** within a VCSEL **1701**. The sensor **100j** further includes an n-side contact **1702** that is coupled to the n-region of each VCSEL **1701** in the array as well as a p-side contact **1704** that is coupled to the p-region of each VCSEL **1701**.

[0086] FIGS. **18A** and **18B** each illustrate various embodiments of one of the VCSELs **1701** illustrated in FIG. **17**. FIG. **18A** illustrates a cross-sectional view through line B' of an example of a VCSEL **1701**, denoted herein as **1701a**, in the sensor **100j** illustrated in FIG. **17**. The VCSEL **1701a** includes an intrinsic semiconducting material **102**, and the intrinsic semiconducting material **102** is n-doped to form a photodetector **104**. The photodetector **104** functions as an n-type lower Bragg reflector. A quantum well **1802** is positioned on the photodetector **104**, and the quantum well **1802** may include an AlGaIn, GaN, InGaIn, and/or N epilayer. The quantum well **1802** defines an opening **1803**, which includes a p-doped region **1804** that is positioned on the photodetector **104**. The p-doped region **1804** functions as p-type upper Bragg reflector.

[0087] The n-side contact **1702**, which is shown in FIG. **17**, is coupled to the photodetector **104**. Similarly, the p-side contact **1704**, which is also shown in FIG. **17**, is coupled to the p-doped region **1804** of the VCSEL **1701**. Also, each VCSEL **1701** is coupled in parallel to a 3 V power supply. In operation, photons **110** in the mid infrared range are absorbed by the photodetector **104** of a VCSEL **1701**, which creates photo-carriers in the photodetector **104**, changing the carrier density. The change in carrier density alters the reflectivity and the index of refraction of the photodetector **104**. Additionally, the change in carrier density alters the resistivity of the photodetector **104**.

[0088] The combination of change in reflectivity and resistivity modulates the emission of the VCSEL **1701**. Further, the absorption of photons **110** effectively changes the overall Q of the laser cavity and modulates the emission of the VCSEL **1701**. In some embodiments, an electrical bias may be applied to one or more of the VCSELs **1701**. Including an array of VCSELs **1701** in a sensor **100** reduces the temperature range of operation of a photodetector **104** to between 0° C. and 40° C.

[0089] An insulating material **1808**, such as a SiO₂ passivation layer, is deposited on the epilayers **1806** by a plasma-enhanced chemical vapor deposition (PECVD) process. The insulating material **1808** is deposited at a low temperature to prevent inter-diffusion of electrons within the quantum well **1802** of the VCSEL **1701**. For example, the PECVD process

may be at temperatures as low as 300° C. for two minutes to deposit 2 microns SiO₂. The shorter the time and temperature, the less damage will occur to the quantum well **1802**. The insulating material **1808** does not cover the p-doped region **1804** and may be etched to provide an opening.

[0090] The doping of the photodetector **104** may be accomplished by standard semiconductor processes such as ion implantation, spin-on doping, and/or other forms of doping. The depth of the dopant may be controlled during the ion implantation process and/or through subsequent thermal anneal treatments. The thermal anneal treatments move the dopants from interstitial sites within the material to place the dopant atoms within the lattice. In the lattice, the dopant has a narrow frequency response range. When the dopant is located in an interstitial site of the intrinsic semiconducting material **102**, the photodetector **104** will have a broadened frequency response relative to the response within the lattice. In some embodiments, the doping may be accomplished by a laser doping technique instead, which will be described below in connection a laser doping system illustrated in FIG. **18A**.

[0091] FIG. **18B** illustrates a cross-sectional view through line B' of an example of a VCSEL **1701**, denoted herein as **1701b**, in the sensor **100j** illustrated in FIG. **17**. The VCSEL **1701b** is similar to the VCSEL **1701a** illustrated in FIG. **18A** in that the quantum well **1802** is positioned on the photodetector **104**. However, in the VCSEL **1701b** illustrated in FIG. **18A**, the p-side contact **1704** covers the insulating layer **1808** and at least a portion of the p-doped region **1804**. The A-side contact **1704** further defines an opening **1818** that exposes the p-doped region **1804**.

[0092] FIG. **19** is a block diagram illustrating an embodiment, among others, of a system **1900** for optically reading an embodiment of a sensor **100**, denoted herein as **100k**. The system **1900** includes an Mid-Wave Infra-Red (MWIR) lens **1902**, the sensor **100k**, a first lens **1904** (denoted herein as **1904a**), a plate **1906** including at least two pinholes **1907** (denoted herein as **1907a** and **1907b**), a light emitting diode (LED) **1905**, a second lens **1904** (denoted herein as **1904b**), and a charge coupled device (CCD) **1908** coupled to a complementary metal oxide semiconductor (CMOS) circuit **1910**. The sensor **100k**, the first lens **1904a**, the plate **1906**, the second lens **1904b**, and the CCD **1908** are each spaced by $1/f$, wherein the frequency is associated with the wavelength of the received light as would be understood by a person of skill in the art.

[0093] The sensor **100k** includes an array of photodetectors **104** that form a focal plane array (FPA). The LED **1905** is useful for acquiring a response from the sensor **100k**, and the LED **1905** is positioned to receive light transmitted through one of the pinholes **1907** (e.g., **1907a**) from the light that pass through the sensor **100k** and are focused by the first lens **1904a**. The light that pass through another pinhole **1907** (e.g., **1907b**) are received by the second lens **1904b**, which transmits the light to the CCD **1908**.

[0094] For example, light are received and focused by the MWIR lens **1902**, which transmits the light to the sensor **100k**. The light pass through the sensor **100k** to the first lens **1904a**, and the first lens **1904a** focuses and transmits the light to the pinholes **1907a**, **1907b** in the plate **1906**. The system **1900** can function as an uncooled wideband camera at various wavelengths, such as shortwave infrared (SWIR), midwave infrared (MWIR), and longwave infrared (LWIR) wavelengths.

[0095] The sensitivity of the sensor **100k** to wavelengths in different ranges can be controlled according to the dopant energy levels of the photodetectors **104**. Also, in some embodiments, a sensor **100k** including a multiwave band FPA is fabricated by doping the photodetectors **104** with multiple dopants of different energy levels. The multiple responses of the multiwave band FPA can be acquired using a plurality of LEDs **1905** that are sensitive to different wavelengths, the CCD **1908**, and signal processing to decouple the signals of the LEDs **1905**.

[0096] The system **1900** may eliminate a need for a custom readout integrated circuit (ROIC), and the system **1900** can be optimized independently from an ROIC. Additionally, the system **1900** (excluding the CMOS circuit **1910** does not require power. Further, the system **1900** presents no bottleneck to the readout data rate, and the system **1900** is scalable to multi-megapixel resolution. The scalability is merely limited by photolithography.

[0097] FIG. **20** is a block diagram illustrating an embodiment of a laser doping system **2000**. The laser doping system **2000** may be used to dope an intrinsic semiconducting material **102** to form a photodetector **104**. The laser doping system **2000** dopes the intrinsic semiconducting material **102** provided in a processing chamber **2004**. The processing chamber **2004** is positioned on a micro stage **2006**, which itself is positioned on a linear stage **2008**. The micro stage **2006** and the linear stage **2008** are useful for adjusting the position of the intrinsic semiconducting material **102** with respect to the position of a laser beam **2010** emitted by a laser **2012**.

[0098] In some embodiments, the laser **2012** is, for example, a neodymium-doped yttrium aluminum garnet (Nd:YAG) laser, which emits a laser beam **2010** (i.e., light) having a wavelength of about 1064 nm. The laser beam **2010** may be frequency doubled to generate laser beam **2010** having a wavelength of about 532 nm. In some embodiments, the laser **2012** is an excimer laser including an excimer of, for example, ArF, KrF, or XeF that emits a laser beam **2010** having a wavelength of 193 nm, 248 nm, and 351 nm, respectively.

[0099] The laser beam **2010** emitted by the laser **2012** is reflected by a bending mirror **2014** to pass through a lens **2016** onto the intrinsic semiconducting material **102** in the processing chamber **2004**. The processing chamber **2004** is mechanically coupled to a bubbler **2018**, and a flow meter **2020** controls the communication of gases and/or liquids between the processing chamber **2004** and the bubbler **2018**. A diffusion pump **2021** and a mechanical pump **2023** are also mechanically coupled to the processing chamber **2004**. In some embodiments, the bubbler **2018** is positioned on the linear stage **2008**.

[0100] The bubbler **2018** is sized and dimensioned to hold a dopant containing liquid **2022** while providing space for holding air at the top of the bubbler **2018**. The bubbler **2018** is positioned on the heater **2019**, and the bubbler **2018** is also mechanically coupled to a carrier gas source **2024** by a gas conducting pipe **2025**, which is partially submerged in the dopant liquid **2022**. The carrier gas provided by the carrier gas source **2024** may be one or more of many inert gases. For example, the carrier gas may include one or more of the following gases: argon, helium, nitrogen, neon, krypton, xenon, and/or radon.

[0101] FIG. **21** is a flowchart showing an example of a method **2100** of laser doping an intrinsic semiconducting material **102** using the laser doping system **2000**. In box **2102**, an intrinsic semiconducting material **102** is provided in a

processing chamber **2004**, and the intrinsic semiconducting material **102** has a lattice. In box **2104**, a carrier gas is communicated from a carrier gas source **2024** to a bubbler **2018**. The dopant carrying gas **2017** is communicated from the bubbler **2018** to the processing chamber **2004** as permitted by the flow meter **2020**. The bubbler **2018** includes a dopant liquid **2022**, which includes a dopant.

[0102] In box **2106**, carrier gas bubbles **2026** are formed in the dopant liquid **2022** in the bubbler **2018**, and in box **2108**, a dopant carrying gas **2017** is formed from the carrier gas bubbles **2026**. The dopant carrying gas **2017** carries the dopant included in the dopant liquid **2022**. In box **2110**, the dopant carrying gas **2017** is communicated to the processing chamber **2004**, which houses the intrinsic semiconducting material **102**.

[0103] In box **2112**, a laser beam **2010** is transmitted to the intrinsic semiconducting material **102**, which is in the presence of a dopant carrying gas **2017** in the processing chamber **2004**. The laser beam **2010** drives the dopant carried by the dopant carrying gas **2017** into the lattice of the intrinsic semiconducting material **102**. The laser beam **2010** heats the intrinsic semiconducting material **102** in the presence of the dopant carrying gas **2017** causing the dopant to thermally diffuse into the intrinsic semiconducting material **102** at the position where the laser beam **2010** heated the intrinsic semiconducting material **102**.

[0104] It should be noted that ratios, concentrations, amounts, and other numerical data may be expressed herein in a range format. It is to be understood that such a range format is used for convenience and brevity, and thus, should be interpreted in a flexible manner to include not only the numerical values explicitly recited as the limits of the range, but also to include all the individual numerical values or sub-ranges encompassed within that range as if each numerical value and sub-range is explicitly recited. To illustrate, a concentration range of “about 0.1% to about 5%” should be interpreted to include not only the explicitly recited concentration of about 0.1 wt % to about 5 wt %, but also include individual concentrations (e.g., 1%, 2%, 3%, and 4%) and the sub-ranges (e.g., 0.5%, 1.1%, 2.2%, 3.3%, and 4.4%) within the indicated range.

[0105] The term “about” can include $\pm 1\%$, $\pm 2\%$, $\pm 3\%$, $\pm 4\%$, $\pm 5\%$, $\pm 6\%$, $\pm 7\%$, $\pm 8\%$, $\pm 9\%$, or $\pm 10\%$, or more of the numerical value(s) being modified. In addition, the phrase “about ‘x’ to ‘y’” includes “about ‘x’ to about ‘y’”.

[0106] It should be emphasized that the above-described embodiments of the present disclosure are merely possible examples of implementations, merely set forth for a clear understanding of the principles of the disclosure. Many variations and modifications may be made to the above-described embodiment(s) of the disclosure without departing substantially from the spirit and principles of the disclosure. All such modifications and variations are intended to be included herein within the scope of this disclosure and the present disclosure and protected by the following claims.

Therefore, at least the following is claimed:

- 1.** A sensor comprising:
 - an array of photodetectors, wherein the reflectance of each of the photodetectors is a function of the number of photons incident on the respective photodetector; and
 - an electrical insulator positioned between one of the photodetectors and another one of the photodetectors to reduce diffusion of electrons therebetween.
- 2.** The sensor of claim **1**, wherein the electrical insulator is at least one of silicon dioxide, a via trench, and a metal coupled to ground.

3. The sensor of claim **1**, wherein at least one of the photodetectors includes gallium doped silicon carbide.

4. The sensor of claim **1**, wherein the each photodetector includes a doped region of an intrinsic semiconducting material.

5. The sensor of claim **4**, wherein the intrinsic semiconducting material is one of silicon carbide (SiC), gallium nitride (GaN), silicon (Si), and gallium arsenide (GaAs).

6. The sensor of claim **4**, wherein the intrinsic semiconducting material is doped with at least one of the following dopants: gallium (Ga), boron (B), aluminum (Al), indium (In), and thallium (Tl).

7. The sensor of claim **1**, wherein the photodetector includes at least two acceptor energy bands, each energy band being associated with a respective one of two dopants.

8. The sensor of claim **7**, wherein the energy difference between the two acceptor energy bands corresponds to photons having a frequency of about 5 terahertz or about 2.5 terahertz.

9. The sensor of claim **7**, wherein at least one of the photodetectors is biased to promote at least some of the electrons in a valence energy band in the least one of the photodetectors to one of the two acceptor energy bands.

10. The sensor of claim **1**, further comprising an array of avalanche photodiodes, wherein each avalanche photodiode includes a respective one of the photodetectors.

11. The sensor of claim **10**, wherein each avalanche photodiode is reverse biased.

12. The sensor of claim **1**, wherein at least one of the photodetectors is doped to absorb photons having a frequency of about 5 terahertz or about 2.5 terahertz.

13. The sensor of claim **1**, wherein an optically-transparent conductive film is positioned on at least one of the photodetectors.

14. The sensor of claim **1**, wherein the photodetector is laser doped.

15. The sensor of claim **1**, further comprising an array of vertical cavity surface emitting lasers (VCSELs), each VCSEL including a respective one of the photodetectors as a Bragg reflector.

16. The sensor of claim **1**, further comprising an array of laser sources and an array of photodiodes, each photodiode including a respective one of the photodetectors.

17. The sensor of claim **16**, wherein each laser source is coupled in parallel to a respective one of the photodiodes.

18. The sensor of claim **17**, wherein each laser source is coupled in series to a respective one of the photodiodes.

19. The sensor of claim **1**, wherein the array includes a first plurality of photodetectors doped to absorb photons corresponding to a first frequency and a second plurality of photodetectors doped to absorb photons corresponding to a second frequency.

20. A method of sensing photons, the method comprising: reflecting a portion of a laser beam using a photodetector; absorbing a plurality of photons incident upon the photodetector, thereby increasing a carrier concentration of the photodetector; and reflecting a greater portion of the laser beam using the photodetector responsive to the absorption of the photons.

21. The method of claim **20**, further comprising transmitting the laser beam to the photodetector.

22. The method of claim **20**, further comprising detecting a power associated with the reflected portion of the laser beam using a power meter.

23. The method of claim **22**, further comprising detecting an increase in the power with the reflected greater portion of the laser beam to a power meter.

24. The method of claim **20**, further comprising redirecting the reflected laser beam to the power meter using a dichroic mirror.

25. The method of claim **20**, wherein the photodetector includes gallium doped silicon carbide.

26. A system comprising:

a sensor including a photodetector, wherein the reflectance of the photodetector is a function of the number of photons absorbed by the photodetector; and

a power meter configured to measure changes in a power of a laser beam reflected by the photodetector.

27. The system of claim **26**, further comprising a dichroic mirror that redirects the reflected laser beam to the power meter.

28. The system of claim **26**, wherein the photodetector includes gallium doped silicon carbide.

29. The system of claim **28**, wherein the sensor further comprises:

a converter layer deposited on the photodetector, and an attenuator layer deposited on the converter layer.

30. The system of claim **29**, wherein the converter layer includes an n-type wide bandgap material having a high capture cross section.

31. The system of claim **29**, wherein the attenuator layer attenuates the velocity of incident particles or radiation.

32. The system of claim **29**, wherein the sensor further comprises an absorber layer deposited on the attenuator layer.

33. The system of claim **29**, wherein the absorber layer includes at least one of zirconium dioxide (ZrO_2), W_2O_3 , boron carbide (BC), boron nitride (BN) and gadolinium carbide (GdC)

34. A laser resonator comprising:

a reflective mirror;

a photodetector positioned opposite the reflective mirror;

a lasing medium positioned between the reflective mirror and the photodetector, wherein the reflectance of the photodetector is a function of the number of photons absorbed by the photodetector, and an intensity of a laser beam emitted by the laser resonator is a function of the reflectance of the photodetector.

35. The laser resonator of claim **34**, wherein the photons are transmitted to the laser resonator through a dichroic mirror, and the dichroic mirror redirects the laser beam emitted by the laser resonator.

36. The laser resonator of claim **34**, wherein the photodetector includes gallium doped silicon carbide.

37. A method of laser doping an intrinsic semiconducting material, the method comprising:

providing a semiconducting material having a lattice; and transmitting a laser beam to the semiconducting material in the presence of a dopant carrying gas carrying a dopant, the laser beam driving the dopant into the lattice of the semiconducting material.

38. The method of claim **37**, further comprising communicating a carrier gas from a carrier gas source to a bubbler, the bubbler including a dopant liquid.

39. The method of claim **38**, wherein the carrier gas includes at least one of the following inert gases: argon, helium, nitrogen, neon, krypton, xenon, and radon.

40. The method of claim **38**, further comprising forming carrier gas bubbles in the dopant liquid using the bubbler.

41. The method of claim **40**, further comprising forming the dopant carrying gas from the carrier gas bubbles in the dopant liquid.

42. The method of claim **37**, wherein the semiconducting material is provided in a processing chamber, the method further comprising communicating the dopant carrying gas from a bubbler to the processing chamber.

43. The method of claim **37**, wherein the dopant is gallium and the semiconducting material is silicon carbide.

44. A method of fabricating a vertical cavity surface emitting laser (VCSEL), the method comprising:

providing an intrinsic semiconducting material having a top surface and a bottom surface;

doping the intrinsic semiconducting material to form a photodetector;

depositing at least one epilayer on the top surface of the doped intrinsic semiconducting material;

depositing a quantum well layer on the at least one epilayer;

depositing a buffer layer on the quantum well layer;

forming a pattern layer on the bottom surface of the intrinsic semiconducting material;

wet etching the intrinsic semiconducting material according to the pattern layer, wherein the at least one epilayer provides an etch stop for wet etching the intrinsic semiconducting material, wherein the wet etching forms a cavity;

depositing a distributed Bragg reflector layer in the cavity; and

depositing an optically-transparent conductive film on the distributed Bragg reflector layer to form a p-side contact.

45. The method of claim **44**, wherein the intrinsic semiconducting material is silicon carbide.

46. The method of claim **44**, wherein the at least one epilayer includes an $Al_xGa_{(1-x)}N$ epilayer, wherein x is within 0.7-0.2.

47. The method of claim **46**, wherein the at least one epilayer also includes a GaN epilayer.

48. The method of claim **47**, wherein the at least one epilayer also includes an AlN epilayer.

49. The method of claim **44**, wherein the quantum well layer includes InGaN.

50. The method of claim **44**, wherein the buffer layer includes GaN.

51. A system comprising:

a sensor including an array of photodetectors that form a focal plane array, wherein at least one of the photodetectors includes gallium-doped silicon carbide; and

a light emitting diode (LED) positioned to receive light transmitted by the sensor.

52. The system of claim **51**, further comprising: a midwave infrared (MWIR) lens, wherein the sensor is positioned to receive light transmitted through the MWIR lens.

53. The system of claim **51**, wherein the LED is coupled to a plate, wherein the plate includes at least two pinholes, and light transmitted through one of the pinholes is received by the LED.

54. The system of claim **53**, wherein a first lens is positioned between the sensor and the plate.

55. The system of claim **53**, wherein a charge coupled device (CCD) is positioned to receive light transmitted through the other pinhole of the plate.

56. The system of claim **55**, wherein the charge coupled device (CCD) is positioned to receive light transmitted through the other pinhole of the plate, wherein a second lens is positioned between the plate and the CCD.